Supplementary Information for:

A blood-brain penetrant RNA-targeting small molecule triggers elimination of r(G_4C_2)^{exp} in c9ALS/FTD via the nuclear RNA exosome

Jessica A. Bush[1], Samantha M. Meyer[1], Rita Fuerst[1], Yuquan Tong[1], Yue Li[1], Raphael I. Benhamou[2], Haruo Aikawa[1], Patrick R. A. Zanon[1], Quentin M. R. Gibaut[1], Alicia J. Angelbello[1], Tania F. Gendron[3], Yong-Jie Zhang[3], Leonard Petrucelli[3], Torben Heick Jensen[4], Jessica L. Childs-Disney[1], and Matthew D. Disney[1,5,*]

[1] Department of Chemistry, The Scripps Research Institute and UF Scripps Biomedical Research, 130 Scripps Way, Jupiter, FL 33458 USA; [2] Institute of Drug Research, The School of Pharmacy, Faculty of Medicine, The Hebrew University of Jerusalem, Jerusalem, Israel [3] Department of Neuroscience, Mayo Clinic, 4500 San Pablo Road, Jacksonville, FL 32224 USA; [4] Department of Molecular Biology and Genetics, Aarhus University, C.F. Møllers Allé 3 (Building 1130), DK-8000 Aarhus C, Denmark; [5] Department of Neuroscience, The Scripps Research Institute and UF Scripps Biomedical Research, 130 Scripps Way, Jupiter, FL 33458 USA;

*Author to whom correspondence is addressed; Email: disney@scripps.edu

This PDF file includes:

- Detailed Methods for all experimental procedures
- Supplementary Text Figs. S1 to S18
- Tables S1 to S9
- References for SI reference citation

EXTENDED METHODS

GENERAL

Oligonucleotides. RNAs and 5'-biotinylated oligonucleotides were purchased from Dharmacon, Inc. (GE Healthcare) and deprotected following the manufacturer's recommended protocol. After desalting using PD-10 columns (GE Healthcare), oligonucleotide concentration was determined by measuring absorbance at 260 nm at 90 °C by UV/Vis spectrophotometry using a Beckman Coulter DU800 UV/Vis spectrophotometer. Extinction coefficients for RNAs were provided by Dharmacon. The sequences of all RNA oligonucleotides are provided in **Table S1**. DNA oligonucleotides (**Table S2**) were purchased from Integrated DNA Technologies (IDT), Inc. with standard desalting provided by the manufacturer and were used without further purification.

IN VITRO METHODS

Microscale thermophoresis (MST). MST measurements were performed on a Monolith NT.115^{Pico} system (NanoTemper Technologies) with the 5'- Cy5-labeled oligonucleotides reported in **Table S1**. Samples were prepared as previously described (1). Briefly, the RNA or DNA of interest (5 nM) was prepared in 1× Folding Buffer (8 mM Na_2HPO_4, pH 7.0185 mM NaCl, and 1 mM EDTA) and folded by heating at 90 °C for 5 min and slowly cooling to room temperature. After cooling, Tween-20 was added to a final concentration of 0.05% (v/v). Compound was then added to the highest final concentration indicated, followed by 1:1 serial dilutions with 1× Folding Buffer containing 5 nM folded nucleic acid, 0.05% (v/v) Tween-20, and the same concentration of DMSO as present in the first sample. Samples were incubated for 30 min at room temperature and then loaded into premium capillaries (NanoTemper Technologies). The following parameters were used on the Monolith NT.115^{Pico} system: 10% LED, 20-80% MST power, Laser-On time = 30 s, Laser-Off time = 5 s. Fluorescence was detected using excitation wavelengths of 605–645 nm and emission wavelengths of 680–685 nm. The resulting data were analyzed by

thermophoresis analysis and fit using the quadratic binding equation in the MST analysis software (NanoTemper Technologies). Dissociation constants were then calculated using Equation 2:

$$K_d = \frac{unbound+(bound-unbound)}{2} * ([nucleic\ acid] + [\mathbf{1}] + K_d\sqrt{([nucleic\ acid] + [\mathbf{1}] + K_d)^2 - 4([nucleic\ acid] * [\mathbf{1}])} \quad \text{Eq. 2}$$

where K_d is dissociation constant, [nucleic acid] is the concentration of the nucleic acid of interest, and [**1**] is the concentration of compound **1**. The reported K_d values are an average of three independent experiments.

In vitro **Chemical Cross-linking and Isolation by Pull-Down (Chem-CLIP) and Competitive Chemical Cross-linking and Isolation by Pull-Down (C-Chem-CLIP).** The RNA repeat $r(G_4C_2)_8$ was 5'-end labeled with [γ-^{32}P] ATP and T4 polynucleotide kinase and gel purified as previously described (2). The radioactively labeled RNA was folded in 1× Folding Buffer at 95 °C for 1 min then allowed to slowly cool to room temperature. Chem-CLIP probe **35** and **36**, prepared in DMSO, were added to the folded RNA to a final concentration of 10, 50, 100, 500, 1000, or 5000 nM. RNA-compound samples were incubated at 37 °C for 18 h. For C-Chem-CLIP studies, the parent compound **1** (0, 100, 500, 1000, 5000 nM) was incubated with RNA for 1 h before addition of the Chem-CLIP probe **35** (500 nM). Following incubation for 18 h at room temperature, samples were photo cross-linked irradiation with UV light (365 nm) for 15 min with UVP Crosslinker and then clicked onto biotin azide (1.0 µL, 10 mM; Sigma Catalog #: 762024) by incubating in 1× Click Buffer (25 mM HEPES, pH 7.1, 250 mM sodium ascorbate, 10 mM $CuSO_4$, and 50 mM THPTA (tris-hydroxypropyltriazolylmethylamine)) for 6 h at 37 °C. Samples were then captured with 20 µL of streptavidin-agarose beads (Sigma-Aldrich; washed 3 times and resuspended in 1× PBS) by incubation for 1 h at room temperature. Following incubation, beads were washed three times with 1× PBS supplemented with 0.1% (v/v) Tween-20 and centrifuged.

The amounts of radioactivity in the supernatant and associated with the beads were quantified with a Beckman Coulter LS6500 Liquid Scintillation Counter.

Time Resolved-Fluorescence Resonance Energy Transfer (TR-FRET). The TR-FRET assay was performed *in vitro* as previously described (1). Briefly, 5′-biotinylated r$(G_4C_2)_8$ (80 nM final) was folded in 1× TR-FRET Folding Buffer (20 mM HEPES, pH 7.5, and 200 mM NaCl) by heating at 95 °C for 5 min followed by slowly cooling to room temperature. The buffer was then adjusted to 1× TR-FRET Assay Buffer (20mM Hepes, pH 7.5, 10mM NaCl, 2mM $MgCl_2$, 2mM $CaCl_2$, 5mM DTT, 0.1% BSA, and 0.05% Tween-20) and hnRNP H-His_6 was added to a final concentration of 75 nM. The sample was allowed to equilibrate at room temperature for 15 min, and then the compound of interest was added. After 15 min, strepatividin-XL665 (cisbio Bioassays) and anti-His_6-Tb (cisbio Bioassays) were added to final concentrations of 40 nM and 0.44 ng/μL, respectively, in a total of 10 μL. The samples were incubated for 15 min at room temperature in the dark and then transferred to a well of a white 384-well plate. Time-resolved fluorescence was measured on a Molecular Devices SpectraMax M5 plate reader. Fluorescence emission from anti-His_6-Tb was measured using an excitation wavelength of 345 nm and an emission wavelength of 545 nm followed by a measurement of FRET using an excitation wavelength of 345 nm and an emission wavelength of 665 nm, with a 200 μs evolution time, and a 1500 μs integration time. The ratio of fluorescence intensity at 545 nm and 665 nm, as compared to the ratios in the absence of ligand and in the absence of RNA, was used for calculation of percent displacement of hnRNP H.

CELLULAR METHODS

Cell Culture. Please see the main text for details regarding cell culture and compound treatment.

Differentiated spinal neurons (iPSNs) were derived from iPSCs (**Table S5**) using a previously reported method with modifications (3, 4). Briefly, 100 mm diameter dishes were coated with Matrigel, and iPSCs were grown until they reached ~30-40% confluency. Neuroepithelial differentiation was first induced by replacing the iPSC Basal Medium with Stage 1 Differentiation Medium [47.5% IMDM (Iscove's Modified Dulbecco's Medium; Life Technologies), 47.5% Ham's F-12 Nutrient Mix (Life Technologies), 1% NEAA (Non-Essential Amino Acids; (Life Technologies), 2% B27 (Invitrogen), 1% N2 (Invitrogen), 1% Penicillin-Streptomycin Solution, 0.2 μM LDN193189 (Stemgent), 10 μM SB431542 (STEMCELL Technologies) and 3 μM CHIR99021 (Sigma-Aldrich)]. Fresh Stage 1 Medium was added for 6 days, after which the cells were detached with Accutase (STEMCELL Technologies) and seeded into 6-well plates (1.5×10^6 cells/well) in 3 mL of Stage 2 Differentiation Medium [Stage 1 medium supplemented with 0.1 μM All-trans retinoic acid (Sigma-Aldrich) and 1 μM smoothened agonist (SAG; Cayman Chemicals)]. Cells were maintained in Stage 2 Medium with medium replaced daily until Day 11. On Day 12, the Stage 2 Medium was removed and replaced with Stage 3 Differentiation Medium [47.5% IMDM, 47.5% Ham's F-12 Nutrient Mix, 1% NEAA, 2% B27, 1% N2, 1% Penicillin-Streptomycin solution, 0.1 μM Compound E (Millipore; Catalog #: 565790), 2.5 μM DAPT (Sigma-Aldrich), 0.1 μM db-cAMP (Millipore), 0.5 μM All-trans retinoic acid, 0.1 μM SAG, 20 ng/mL ascorbic acid, 10 ng/mL brain-derived neurotrophic factor (BDNF; STEMCELL Technologies), and 10 ng/mL glial cell line-derived neurotrophic factor (GDNF; STEMCELL Technologies)], which was replaced with fresh medium every 3-4 days.

Beginning on Day 15 of differentiation, cells were treated with compound diluted in Stage 3 Differentiation Medium with a final concentration of <0.1% (v/v) DMSO. Fresh medium

containing compound was replenished every 3-4 days until cells reached full maturity at Day 32, after which cells were harvested for analysis.

Assessing DNA Damage of Lead Molecules. HEK293T cells (~8000 cells/well) were seeded into 96-well plates and incubated overnight. Compounds (1 µL) were then added directly to the culture medium (1% (v/v) final DMSO concentration), and cells were incubated for 24 h. After treatment, DNA damage was assessed by measuring phosphorylation of serine 139 (Ser139) of γ-H2AX using a FRET-based Phospho-γ-H2AX (Ser139) Cellular Kit (Cisbio), according to the manufacturer's protocol. Fluorescence emission was read at two different wavelengths (665nm and 620nm) on a Molecular Devices SpectraMax M5 plate reader. For each sample, the ratio of the fluorescence of the acceptor (FRET; 665 nm) to the fluorescence of the donor (620 nm) was calculated. The ratio of compound-treated cells was compared to vehicle-treated cells (normalized to 1).

Cell Viability. Patient-derived LCLs were seeded in 96-well plates (~10^4 cells/well) and incubated overnight. They were then treated with compound in growth medium for 48 h. Cell viability was measured using the CellTiter-Fluor™ Cell Viability Assay (Promega) per the manufacturer's protocol. For iPSCs, cells were seeded in Matrigel-coated 6-well plates and grown in Basal Medium. After 24 h, fresh medium containing compound was added for an additional 48 h. Following treatment, cell viability was measured by AlamarBlue™ Cell Viability Reagent (DAL1025, Thermo Fisher Scientific), per the manufacturer's protocol.

Target Profiling by ASO-Bind-Map. Patient-derived LCLs were plated at 1×10^6 cells per well in a 6-well plate and incubated overnight in growth medium. The cells were first treated with compound (final concentration of 0.1% (v/v) DMSO) for 24 h. Following compound treatment, the cells were transfected with 100 nM ASO using Lipofectamine RNAiMax (Life Technologies) and incubated for another 24 h. Total RNA was extracted using a Quick-RNA Miniprep Kit (Zymo Research), and RT-qPCR was performed as described below.

Cellular Chem-CLIP. Patient-derived iPSCs were cultured in 6-well plates as described in "**Target Profiling by ASO-Bind-Map"**. Cells were treated with Chem-CLIP probe in growth medium (final concentration of 0.1% (v/v) DMSO) for 24 h. Following treatment, cells were washed with 1× Dulbecco's Phosphate-Buffered Saline (DPBS; Fisher Scientific), and cross-linking was performed by UV irradiation with 365 nm light for 10 min. After cross-linking, the cells were lysed with RNA Lysis Buffer (from a Zymo Quick-RNA Miniprep Kit), and total RNA was extracted using a Quick-RNA Miniprep Kit (Zymo Research), per the manufacturer's protocol. Next, a click onto disulfide agarose azide beads (Click Chemistry Tools) was performed at 37 °C for 2 h in 1× Click Buffer (described above). After washing the beads 6 times with High Salt Wash Buffer (10 mM Tris-HCl pH 7.0, 1 mM EDTA, 4 M NaCl, and 0.2% (v/v) Tween-20), the pulled-down RNA was eluted from the beads using a 1:1 mixture of TCEP (200 mM) and K_2CO_3 (600 mM), with shaking at 37 °C for 30 min, followed by quenching with 400 nM iodoacetamide incubated with shaking at 37 °C for 30 min. The supernatant for each sample was collected, and the RNA was purified with RNA Clean XP beads (Beckman Coulter) per the manufacturer's recommended protocol. The RNA obtained from pull-down was subjected to RT-qPCR for the determination of *C9orf72* mRNA levels as described below.

Measuring Levels of *C9orf72* Variants by RT-qPCR. LCLs and iPSCs, whether patient-derived or from healthy donors, were seeded into 6-well plates (~10^6 cells in 2 mL of Basal Medium) and incubated overnight at 37 °C. The medium was then replenished and the cells were treated as indicated for a particular experiment. Total RNA was extracted using a Quick-RNA Miniprep Kit (Zymo Research), per the manufacturer's protocol. Reverse transcription was performed using 1 µg of total RNA, as determined by Nanodrop UV spectrophotometer (ThermoFisher), and a qScript™ cDNA Synthesis Kit (Quantabio), per the manufacturer's protocol. RT-qPCR was performed on a QuantStudio™ Real-Time PCR Instrument (Applied Biosystems) using Power SYBR Green Master Mix (Applied Biosystems). Expression levels of

mRNAs were normalized to *GAPDH, β-actin, or 18S* rRNA as indicated. See **Table S2** for a list of primers.

For iPSNs, cells were differentiated to Day 15, as described above, after which cells were replenished with medium containing compound every 3-4 days until reaching Day 32 of differentiation. Total RNA was extracted as described above, and the expression of *C9orf72* variants was determined by RT-qPCR. See **Table S2** for a list of primers.

RNA Sequencing. All sequencing data described in this paper were deposited in Mendeley Data (DOI: 10.17632/k3ph59xrtz.1). Total RNA integrity was confirmed by Agilent 2100 Bioanalyzer RNA nano chip, and the quantity was measured by Qubit 2.0 Fluorometer (Invitrogen). Library preparation was performed using a NEBNext Ultra II Directional RNA kit (NEB, E7760) in combination with a NEBNext rRNA depletion module (NEB, E6310) and an RNA fragmentation module (NEB, E6150S), following the manufacturer's recommendations. Briefly, 200 ng of total RNA was first depleted of ribosomal RNA and then randomly fragmented to a range of 150 to 300 nucleotides. The fragmented RNAs were randomly primed for first-strand cDNA synthesis, and the second strand was synthesized with dUTPs. The strand information is thus preserved by using USER enzyme (Uracil-specific excision reagent). The cDNA was PCR-amplified and pooled in equimolar amounts for loading into a NextSeq 500 v2.5 flow cell. The RNAs were sequenced by using a 2 × 40 bp paired-end method. The output fastq files were aligned using STAR (5), and read counts of specific regions were extracted using samtools (6). The global differential gene expression analysis was performed using featureCounts and Deseq2 (7, 8).

Measuring poly(GP) Levels Using an Electrochemiluminescent Immunoassay. After the indicated treatment period, patient-derived cells were harvested and total protein was extracted into CoIP2 buffer [50 mM Tris-HCL, pH 7.4, 300 mM NaCl, 5 mM EDTA, 1% (v/v) Triton-X 100, 2% (w/v) sodium dodecyl sulfate (SDS), 0.01% Protease and Phosphatase inhibitors

(Fisher Scientific)] by incubating on ice for 5 min followed by sonication (3 s intervals at 35% power for approximately 20 s). Detergent was removed using a Pierce™ Detergent Removal Spin Column 0.5 mL (Thermo Scientific), following the manufacturer's protocol. Protein concentration was measured by Pierce™ Micro BCA Protein Assay Kit (Thermo Scientific), where each sample was measured in triplicate.

Poly(GP) levels were measured an electrochemiluminescent sandwich immunoassay. Briefly, gold 96-well streptavidin SECTOR plates (Meso Scale Discovery) were incubated with 2 μg/mL of biotin-conjugated anti-poly(GP)antibody at 4 °C overnight. After incubation, the wells were washed three times with 1× TBST (Tris-buffered saline containing 0.1% (v/v) Tween-20) and then blocked with a solution of 3% (w/v) bovine serum albumin (BSA) in 1× TBST for 1 h with shaking at room temperature. The plate was washed three times with 1× TBST. Following these washes, 80 μg of cell lysate was added to each well, and the samples were incubated for 2 h with shaking at room temperature. The plates were then washed three times with 1× TBST, followed by addition of 4 μg/mL of Sulfo-conjugated anti-poly(GP) antibody diluted in a solution of 3% (w/v) BSA and incubated at room temperature with shaking for 1 h. After washing once with 1× TBST, 1× MSD GOLD Read Buffer (Meso Scale Discovery) was added to each well, and electrochemiluminescence was measured by a SECTOR Imager (Meso Scale Discovery).

Western Blotting. Protein samples were prepared as described above. Approximately 50 μg total protein was loaded onto a 4-20% Mini-PROTEAN® TGX™ Precast Protein Gel (Bio-Rad) using a Tris-Glycine/SDS Running Buffer (25 mM Tris base, pH 8.3, 190 mM glycine, and 0.1% (w/v) SDS). Following electrophoresis, protein was transferred to a PVDF membrane using a Tris-Glycine Transfer Buffer (25 mM Tris base, pH 8.3, 190 mM glycine, and 20% (v/v) methanol). After transfer, the membrane was blocked with 5% (w/v) non-fat milk in 1× TBST for 30 min with shaking at room temperature. After blocking, the membrane was incubated with an anti-C9orf72 antibody (GeneTex, GTX119776; 1:3000 dilution) in 1× TBST containing 5% (w/v)

non-fat milk overnight at 4 °C. The membrane was then washed three times with 1× TBST and incubated with a 1:2000 dilution of anti-mouse IgG horseradish-peroxidase secondary antibody conjugate (Cell Signaling Technology) prepared in 1× TBST supplemented with 5% (w/v) non-fat milk for 1 h at room temperature with shaking. The membrane was washed three times with 1× TBST, and protein expression was visualized using SuperSignal West Pico Plus Chemiluminescent Substrate (Life Technologies), per the manufacturer's protocol. Relative protein expression was quantified using ImageJ (NIH).

To quantify β-actin expression, the membrane was washed with 1× TBST and stripped using 1× Stripping Buffer (200 mM glycine, pH 2.2, 1% (v/v) Tween-20, and 0.1% (w/v) SDS). Following stripping, the membrane was washed with 1× TBST and blocked with 5% (w/v) non-fat milk in 1× TBST for 30 min at room temperature with shaking. The membrane was then incubated with a 1:5000 dilution of β-actin primary antibody (Cell Signaling Technology) prepared in 1× TBST with 5% (w/v) non-fat milk overnight at 4 ˚C. After incubation, the membrane was washed three times with 1× TBST and incubated with a 1:10,000 dilution of anti-mouse IgG horseradish-peroxidase secondary antibody conjugate (Cell Signaling Technology) prepared in 1× TBST with 5% (w/v) non-fat milk for 1 h at room temperature with shaking. The membrane was washed three times with 1× TBST, and protein expression was visualized using SuperSignal West Pico Plus Chemiluminescent Substrate per the manufacturer's protocol. Relative protein expression was quantified using ImageJ (NIH).

Imaging of RNA Foci in LCLs. For patient-derived lymphoblastoid cells (ND11749), RNA foci containing $r(G_4C_2)^{exp}$ were imaged using RNA fluorescence *in situ* hybridization (FISH) as previously described (9). LCLs were cultured and treated for 4 days as described above. Following treatment, cells were pelleted by centrifugation, washed twice with 1× DPBS, and fixed in 2% paraformaldehyde for 15 min, and washed an additional three times in 1× DPBS. The fixed cells were seeded onto polylysine-coated, glass-bottom 96-well plates, at a density of 1×10^6 cells per well. The cells were again incubated at 37 °C for more than 2 h to ensure adhesion. Then

cells were incubated with 70% ethanol overnight at 37 °C. The next day, cells were washed with 1× DPBS for 15 min at room temperature followed by incubation with 0.1% (v/v) Triton X-100 in 1× DPBS for 5 min at room temperature. The cells were then washed with 40% formamide in 2× Saline Sodium Citrate (SSC) buffer for 15 min at room temperature. Next, the FISH probe [5 ng/μL 5'- TYE563-d(G_2C_4)$_4$]-TYE563 in 40% formamide in 2× SSC supplemented with 2 μg/mL BSA, 330 ng/mL yeast tRNA, and 2 mM vanadyl complex was added to each sample, and the samples were incubated at 37 ºC and 5% CO_2 for 24 h. Following hybridization with the FISH probe, the cells were washed three times in 2× SSC at room temperature for 15 min each, followed by three washes with 1× DPBS for 15 min each. DAPI (1 μg/mL in 1× DPBS) was then added, and samples were incubated for 10 min, followed by washing with three times 1× DPBS at room temperature. The cells were imaged with an Olympus Fluoview 1000 confocal microscope with a 60x objective with ~200 cells counted per treatment group imaging DAPI and Alexa 563.

IN VIVO METHODS

Therapeutic Efficacy in c9ALS/FTD Mouse Models. All animal studies were completed as approved by the Scripps Florida Institutional Animal Care and Use Committee. To determine compound dosing, initial DMPK studies were performed in male C57 Bl/6J mice (n = 3 mice per treatment group). Compound was formulated to a final concentration of 1 mg/mL in a solution of 10% DMSO 90% Saline. A single intraperitoneal (*i.p.*) injection of 10 mg/kg was administered and plasma and brain samples were harvested 120 min following injection for analyte detection to determine compound concentration.

For further studies, mice were treated by daily *i.p.* injection of 10 mg/kg of **1** diluted in 10% (v/v) DMSO / 90% (v/v) saline for a period of two weeks. Mouse weights were recorded over the dosing period. Mice were euthanized 24 h post final dosing (Day 15) when tissues were harvested for study. For studies in both +/+PWR500 and Lutzy transgenic mouse models, post-mortem brain tissue was harvested and sliced sagittally at the midline. The right hemisphere was carried forward to immunohistochemistry studies while the left hemisphere was frozen for RNA and protein analyses (both described below).

+/+PWR500 BAC Mice. A total of 34 mice [22 +/+PWR500 (13 M, 9 F) and 12 WT (6 M, 6 F)], age- and gender-matched and ranging in age from 18-22 weeks old, were used in therapeutic efficacy studies (**Table S7**).

Lutzy BAC Mice. A total of 20 mice [12 +/+Lutzy (4 M, 8 F) and 8 WT (4 M, 4 F) mice, age- and gender-matched and ranging in age from 18-22 weeks old, were used in therapeutic efficacy studies (**Table S8**).

Measuring *C9orf72* Variants by RT-qPCR. Frozen brain tissue was homogenized in 300 µL Tris-EDTA buffer (10 mM Tris-HCl, pH 8.0 and 1 mM disodium EDTA) with 2× Protease and Phosphatase Inhibitors (Research Products International Cat# P50700-1) at 1:5 (w/v) ratio. Triazol LS was added in a 1:3 ratio to 150 µL homogenized tissue, and samples were centrifuged for 15 min at 16,000 rpm. Following centrifugation, the supernatant was collected, and an equal

volume of 100% ethanol was added. The harvested RNA was then purified using a Direct-zol RNA Kit (Zymo Research), per the manufacturer's protocol. RT-qPCR was performed as described above. Expression levels of mRNAs were normalized to mouse *β-actin*. See **Table 2** for a list of primers.

Measuring poly(GP) Levels Using an Electrochemiluminescent Immunoassay. Frozen brain tissue was homogenized in 300 µL Tris-EDTA Buffer with 2× Protease and Phosphatase Inhibitors at 1:5 (w/v) ratio, as was completed for RNA analysis of the tissue. Next, 150 µL of homogenized tissue was mixed with 2× Lysis Buffer [50 mM Tris HCl pH 7.4, 250 mM NaCl, 2% (v/v) Triton X-100, 4% (w/v) SDS, and 1× Protease Inhibitor (Fisher Scientific)]. Brain lysates were sonicated in 1 s on/off intervals at 30% power for 15 s. Protein concentrations were measured in triplicate using a Micro BCA Protein Assay Kit and poly(GP) levels were measured using the electroluminescent immunoassay as described above.

Measuring DPR Levels Using Western Blot Analysis. Protein samples were prepared as described in "Measuring poly(GP) Levels Using an Electrochemiluminescent Immunoassay". Approximately 50 µg total protein was loaded onto a 5-8% acrylamide gel and run in a Tris-Glycine/SDS Running Buffer (25 mM Tris base, pH 8.3, 190 mM glycine, and 0.1% (w/v) SDS). Following electrophoresis, protein was transferred to a PVDF membrane using a Tris-Glycine Transfer Buffer (25 mM Tris base, pH 8.3, 190 mM glycine, and 20% (v/v) methanol). After transfer, the membrane was blocked with 5% (w/v) non-fat milk in 1× TBST for 1 h with shaking at room temperature. After blocking, the membrane was incubated with primary antibody [Millipore; poly(GA): 1:1000, MABN889, or Millipore; poly(GP): 1:1000, ABN455] in 1× TBST containing 5% (w/v) non-fat milk overnight at 4 °C. The membrane was then washed three times with 1× TBST and incubated with a 1:2000 dilution of anti-mouse IgG horseradish-peroxidase secondary antibody conjugate (Cell Signaling Technology) prepared in 1× TBST supplemented with 5% (w/v) non-fat milk for 1 h at room temperature with shaking. The membrane was washed three times with 1× TBST, and protein expression was visualized using SuperSignal West Pico

Plus Chemiluminescent Substrate (Life Technologies), per the manufacturer's protocol. Relative protein expression was quantified using ImageJ (NIH).

To quantify β-actin expression, the membrane was stripped using 1× Stripping Buffer (200 mM glycine, pH 2.2, 1% (v/v) Tween-20, and 0.1% (w/v) SDS). Following stripping, the membrane was washed with 1× TBST and blocked with 5% (w/v) non-fat milk in 1× TBST for 1 h at room temperature with shaking. The membrane was then incubated with a 1:5000 dilution of β-actin primary antibody (Cell Signaling Technology) prepared in 1× TBST with 5% (w/v) non-fat milk overnight at 4 ˚C. After incubation, the membrane was washed three times with 1× TBST and incubated with a 1:10,000 dilution of anti-mouse IgG horseradish-peroxidase secondary antibody conjugate (Cell Signaling Technology) prepared in 1× TBST with 5% (w/v) non-fat milk for 1 h at room temperature with shaking. The membrane was washed three times with 1× TBST, and protein expression was visualized using SuperSignal West Pico Plus Chemiluminescent Substrate per the manufacturer's protocol. Relative protein expression was quantified using ImageJ (NIH).

Immunohistochemistry. Right brain hemispheres (not frozen) were stored in 10% neutral buffered formalin (VWR) for 48 h. Tissue processing, embedding, and sectioning were carried out by the Scripps Florida Histology Core. Tissue was first embedded in paraffin using a Sakura Tissue-Tek VIP5 paraffin processor, sectioned at 4 μm, and mounted on positively charged slides. The slides were stained with primary antibody (see below) on the Leica BOND-MAX platform. After primary staining, slides were subjected to the Leica Refine Detection Kit containing the secondary polymer, DAB chromagen, and counterstain. After dehydration in graded alcohols and clearing in xylene, the slides were cover slipped with a permanent mounting medium, Cytoseal 60 (Thermo Scientific).

Antibodies. NeuN: 1:2000, RRID: AB_177621, Millipore; poly(GA): 1:2000, MABN889, Millipore; poly(GP): 1:5000, ABN455, Millipore; Calbindin: 1:5000, RRID: AB_476894, Millipore; TDP-43: 1:2000, RRID: AB_615042, ProteinTech.

RNA FISH and Immunofluorescence Analyses of Mouse Brain Sections. Right hemispheres were flash-frozen with Optimal Cutting Temperature (OCT; Fisher Scientific) compound in 2-methylbutane in liquid nitrogen. Left hemispheres were harvested for total RNA and protein. Frozen tissue was sectioned into 10 µm thick sections using a cryostat. Slides were then stained as previously described (10). Briefly, frozen sections were fixed in 4% (w/v) paraformaldehyde in 1× DPBS for 20 min and incubated in ice-cold 70% ethanol for 30 min at 4 °C. Once fixed, slides were then incubated in 40% formamide in 2× SSC Buffer for 10 min at room temperature. Slides were blocked in 1× Hybridization Buffer (40% formamide, 2× SSC, 20 µg/mL BSA, 100 mg/mL dextran sulfate, 250 µg/mL tRNA, and 2 mM vanadyl sulfate) for 30 min at 55 °C, then incubated with 200 ng/mL of FISH probe (**Table S1**) in 1× Hybridization Buffer for 3 h at 55 °C. Following hybridization, slides were washed three times in 40% (v/v) formamide in 2× SSC Buffer and washed with 1× DPBS and then co-stained with NeuN (Sigma: MAB377B) as follows. The slide-mounted tissue was permeabilized with 0.5% (v/v) Triton X-100 in 1× DPBS for 15 min at 4 °C and then blocked with 2% goat serum diluted in 1× DPBS [blocking solution] for 1.5 h at 4 °C. Slides were then incubated overnight at 4 °C with anti-NeuN antibody (1:500, MAB377B, Sigma) diluted in the blocking solution. After the slides were washed three times with 1× DPBS, they were incubated with donkey anti-goat IgG conjugated to Alexa Fluor 488 (AbCam, Inc.; diluted 1:500 in 1× DPBS) for 1 h at room temperature. Following incubation, slides were washed three times with 1× DPBS and quenched with 0.25% (w/v) Sudan Black B (Millipore) diluted in 70% ethanol. After washing, slides were dried completely, mounted with mounting medium containing DAPI (Invitrogen), and imaged using a 60× objective on an Olympus Fluoview 1000 confocal microscope.

SYNTHETIC METHODS

Abbreviations: Ac_2O, acetic anhydride; BnCl, benzyl chloride; DCM, dichloromethane; DIPEA, *N*,*N*-diisopropylethylamine; DMF, *N*,*N*-dimethylformamide; DMSO, dimethyl sulfoxide; EDC, *N*-ethyl-*N*'-(3- dimethylaminopropyl)carbodiimide hydrochloride; Et_3N, triethylamine; EtOAc, ethyl acetate; HOBt, 1-hydroxybenzotriazole; HPLC, high performance liquid chromatography; MALDI, matrix-assisted laser desorption/ionization; MeOH, methanol; NaOMe, sodium methoxide; NMR, nuclear magnetic resonance; PEG, polyethylene glycol; TFA, trifluoroacetic acid; THF, tetrahydrofuran; TLC, thin layer chromatography.

General. All commercially available reagents and solvents were used without further purification. All non-aqueous reactions were carried out under argon atmosphere. Reactions were monitored by thin-layer chromatography (TLC Standard Silica Plate from Agela Technologies Catalog #: 97055-788 or Kieselgel 60 F254 glass plates pre-coated with a 0.25 mm thickness of silica gel). Spots were visualized with UV light, and stained with phosphomolybdic acid, Ninhydrin, or Hanessian solution [H_2SO_4 (conc., 22 mL), phosphomolybdic acid (20 g), $Ce(SO_4)_2$ (0.5 g), 378 mL H_2O)].

Column chromatography was performed on an Isolera One (Biotage) with pre-packed silica gel column (Agela Technologies) or HPLC (Waters 2489 and 1525) with SunFire® Prep C18 OBD™ 5 μm column (19×150 mm) and a flow rate: 5 mL/min. Product puritiy was analyzed by HPLC (Waters 2487 and 1525) with SunFire® C18 3.5 μm column (4.6x150 mm) and a flow rate of 1 mL/min.

NMR spectra were recorded on a 400 UltraShield™ (Bruker; 400 MHz for ^1H and 100 MHz for ^{13}C) or Ascend™ 600 (Bruker; 600 MHz for ^1H and 150 MHz for ^{13}C). Chemical shifts are expressed in ppm relative to TMS and residual solvent for ^1H and ^{13}C as internal standards, respectively. Coupling constant (*J* values) are reported in Hertz.

High-resolution mass spectra (HR-MS) were recorded on a 4800 Plus MALDI TOF/TOF Analyzer (Applied Biosystems) using α-cyano-4-hydroxycinnamic acid matrix and TOF/TOF Calibration Mixture (AB Sciex Pte. Ltd.), an Agilent 1260 Infinity LC system-Agilent 6230 TOF (HR-ESI) with a Poroshell 120 EC-C18 column (Agilent, 50 mm x 4.6 mm, 2.7 μm), or an ESI spectrometer at the University of Illinois Urbana-Champaign Mass Spectrometry Laboratory.

Synthetic Procedures

Intermediates i**1-i3** (11, 12), i**5**, i**7**, and compounds **18** and **19** (13) were synthesized as previously reported.

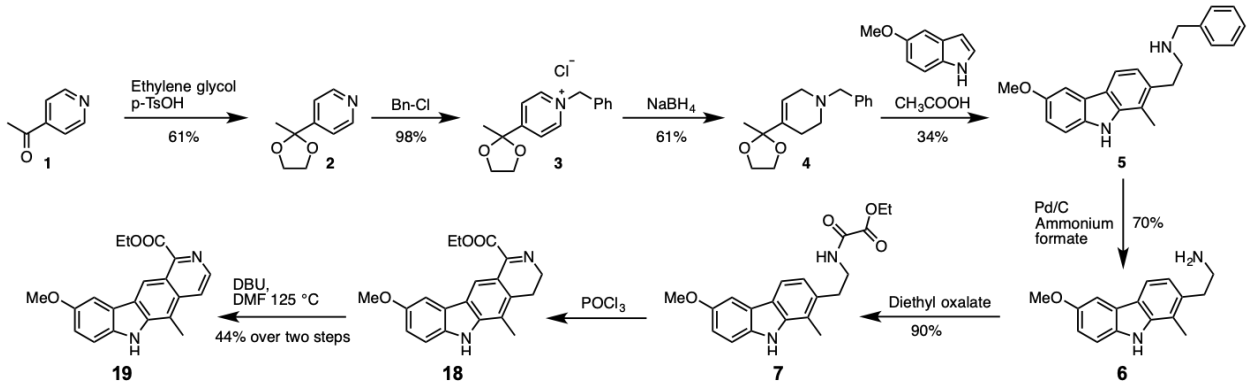

Intermediate i4

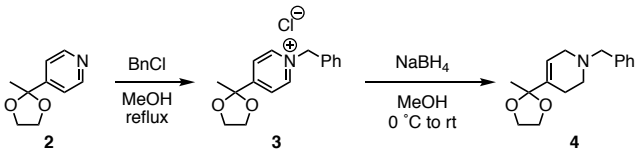

To a solution of i**2** (above scheme) (60 g, 363 mmol) in methanol (250 mL) was added BnCl (46 mL, 400 mmol), and the solution was stirred for 4 h at 80 ˚C. Additional BnCl (25 mL, 217 mmol) was added, and the reaction was stirred overnight at 80 ˚C to drive the reaction to completion. The solvent was evaporated, and the residue was washed with 100 mL of hexanes three times. The resulting crude product was used for the next reaction without further purification.

To a solution of the crude product isolated above in methanol (600 mL) was added $NaBH_4$ (13.7 g, 363 mmol) portion-wise at 0 ˚C. The reaction was removed from the ice bath and stirred for 2 h at room temperature. A 1:1 mixture of MeOH/H_2O (200 mL) was added to the solution at 0 ˚C. The solvent was evaporated, and the crude product was extracted with DCM, washed with sat. $NaHCO_3$ aq and brine, and dried with Na_2SO_4. The desired product was purified by silica gel column (DCM:MeOH=20:1, 1% Et_3N) to give i**4** as a colorless oil (80 g, 309 mmol, 85% over two steps). ^{1}H NMR (600 MHz, $CDCl_3$): δ = 7.36-7.29 (4H), 7.25 (m, 1H), 5.81 (m, 1H), 3.97-3.89 (2H), 3.86-3.79 (2H), 3.59 (s, 2H), 3.04-2.99 (2H), 2.55 (t, *J* = 5.7 Hz, 2H), 2.20-2.13 (2H), 1.45 (s, 3H); ^{13}C NMR (150 MHz, $CDCl_3$): δ = 138.1, 136.3, 129.1, 128.2, 127.0, 120.5, 108.8, 64.3, 62.6, 52.4, 49.5, 24.9, 23.7; HR-MS (MALDI): Calcd. for $C_{16}H_{22}NO_2^+$ $[M+H]^+$: 260.1645; found: 260.1651.

General procedure of aminolysis for the synthesis of compounds 21 – 30.

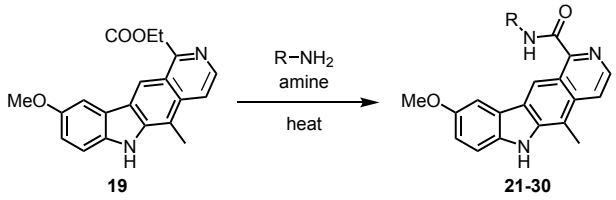

19 **21-30**

Compound **19** (20 mg, 58 μmol, 1.0 eq) was dissolved in the corresponding amine (100 eq), heated to 120 °C, and stirred for 6 h. The reaction mixture was concentrated *in vacuo* and HPLC purified (linear gradient 10-100% acetonitrile/MeOH, 0.1% TFA).

Ethyl-9-methoxy-5,6-dimethyl-6*H*-pyrido[4,3-*b*]carbazole-1-carboxylate (20)

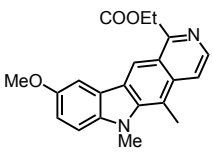

Compound **19** (120 mg, 0.359 mmol, 1.0 eq) was dissolved in DMF (1.8 mL) and cooled to 0 °C. After the addition of NaH (60% suspension in mineral oil, 19 mg, 0.467 mmol, 1.3 eq), the resulting suspension was stirred for 30 min at 0 °C before methyl iodide (25 µL, 0.395 mmol, 1.1 eq) was added. The cooling bath was removed, and the reaction mixture was stirred at room temperature for 12 h. After dilution with DCM (15 mL) and H_2O (10 mL), the product was extracted three times with DCM (10 mL). The combined organic extracts were dried over Na_2SO_4, filtered, and the solvent was removed under reduced pressure. The crude product was purified by flash chromatography (1-10% MeOH in DCM, linear gradient) providing **20** (73 mg) in 58% yield. ^{1}H NMR (400 MHz, $CDCl_3$) δ 9.51 (s, 1H), 8.62 (d, *J* = 6.5 Hz, 1H), 8.28 (d, *J* = 6.5 Hz, 1H), 7.72 (d, *J* = 2.4 Hz, 1H), 7.34 (d, *J* = 8.8 Hz, 1H), 7.29 – 7.22 (m, 1H), 4.68 (q, *J* = 7.2 Hz, 2H), 4.17 (s, 3H), 3.98 (s, 3H), 3.12 (s, 3H), 1.57 (t, *J* = 7.2 Hz, 3H). ^{13}C NMR (101 MHz, $CDCl_3$) δ 166.98, 154.21, 141.80, 139.71, 139.51, 135.02, 127.51, 122.97, 121.09, 119.06, 117.05, 115.41, 111.11, 109.45, 103.99, 62.15, 56.21, 33.61, 14.56, 13.85. HR-MS (ESI) calcd. for $C_{21}H_{21}N_2O_3^+$ $[M+H]^+$: 349.1547; found: 349.1549.

9-methoxy-*N*-(2-methoxyethyl)-5-methyl-6*H*-pyrido[4,3-*b*]carbazole-1-carboxamide (21)

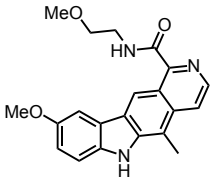

Yield: 20.1 mg, 96%. ^{1}H NMR (400 MHz, CD_3OD) δ 8.74 (s, 1H), 8.05 (d, *J* = 6.8 Hz, 1H), 8.00 (d, *J* = 6.8 Hz, 1H), 7.42 (d, *J* = 2.5 Hz, 1H), 7.30 (d, *J* = 8.7 Hz, 1H), 7.09 (dd, *J* = 2.5, 8.7 Hz, 1H), 3.86 (s, 3H), 3.86 – 3.82 (m, 2H), 3.81 – 3.77 (m, 2H), 3.51 (s, 3H), 2.59 (s, 3H). ^{13}C NMR (176 MHz, CD_3OD) δ 163.08, 154.64, 149.80, 144.04, 137.18, 133.81, 130.80, 129.03, 128.50, 128.04, 122.13, 119.34, 117.79, 117.54, 111.71, 103.84, 70.21, 57.64, 54.92, 47.94, 39.58, 10.84. HR-MS (ESI) calcd. for $C_{21}H_{22}N_3O_3^+$ $[M+H]^+$: 364.1656; found: 364.1679.

9-methoxy-5-methyl-*N*-propyl-6*H*-pyrido[4,3-*b*]carbazole-1-carboxamide (22)

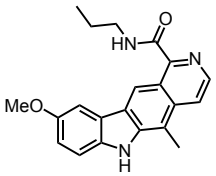

Yield: 13.1 mg, 63%. ^{1}H NMR (700 MHz, CD_3OD) δ 8.99 – 8.87 (m, 1H), 8.18 (s, 2H), 7.68 – 7.57 (m, 1H), 7.45 – 7.37 (m, 1H), 7.23 – 7.14 (m, 1H), 3.92 (s, 3H), 3.64 (t, *J* = 7.2 Hz, 2H), 2.74 (s, 3H), 1.85 (h, *J* = 7.2 Hz, 2H), 1.15 (t, *J* = 7.2 Hz, 3H). ^{13}C NMR (176 MHz, CD_3OD) δ 163.47, 154.76, 150.47, 144.21, 137.38, 133.97, 129.23, 128.17, 122.31, 119.36, 117.86, 117.47, 111.83, 111.72, 103.98, 54.96, 41.81, 22.08, 10.88, 10.56. HR-MS (ESI) calcd. for $C_{21}H_{22}N_3O_2^+$ $[M+H]^+$: 348.1707; found: 348.1696.

***N*-(3-(dimethylamino)propyl)-9-methoxy-5-methyl-6*H*-pyrido[4,3-*b*]carbazole-1-carboxamide (23)**

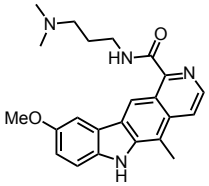

Yield: 20.6 mg, 91%. ^{1}H NMR (400 MHz, CD_3OD) δ 8.84 (s, 1H), 8.16 (d, *J* = 6.7 Hz, 1H), 8.08 (d, *J* = 6.7 Hz, 0H), 7.51 (d, *J* = 2.5 Hz, 1H), 7.35 (d, *J* = 8.7 Hz, 1H), 7.13 (dd, *J* = 2.5, 8.7 Hz, 1H), 3.89 (s, 2H), 3.77 (t, *J* = 6.6 Hz, 3H), 3.44 – 3.35 (m, 2H), 2.99 (s, 6H), 2.66 (s, 3H), 2.31 – 2.12 (m, 2H). ^{13}C NMR (176 MHz, CD_3OD) δ 163.98, 154.64, 149.70, 143.98, 137.29, 133.91, 129.31, 128.02, 122.23, 119.47, 117.74, 117.62, 117.33, 111.73, 111.66, 104.11, 55.37, 54.98, 42.14, 36.71, 24.39, 10.85. HR-MS (ESI) calcd. for $C_{23}H_{27}N_4O_2^+$ $[M+H]^+$: 391.2129; found: 391.2120.

***N*-(2-hydroxyethyl)-9-methoxy-5-methyl-6*H*-pyrido[4,3-*b*]carbazole-1-carboxamide (24)**

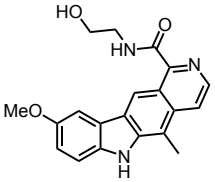

Yield: 11.1 mg, 53%. ^{1}H NMR (600 MHz, CD_3OD) δ 9.00 (s, 1H), 8.30-8.05 (2H), 7.61 (d, *J* = 2.4 Hz, 1H), 7.39 (d, *J* = 8.7 Hz, 1H), 7.16 (dd, *J* = 8.7, 2.5 Hz, 1H), 3.96-3.92 (2H), 3.90 (s, 3H), 3.82-3.76 (2H), 2.73 (s, 3H). ^{13}C NMR (150 MHz, CD_3OD) δ 164.3, 156.3, 151.4, 146.0, 138.7, 135.5, 129.9, 129.2, 123.7, 121.0, 119.6, 119.5, 119.0, 113.4, 113.2, 105.6, 61.2, 56.4, 44.0, 12.3. HR-MS (ESI) calcd. for $C_{20}H_{20}N_3O_3^+$ $[M+H]^+$: 350.1499; found: 350.1515.

***N*-(2-aminoethyl)-9-methoxy-5-methyl-6*H*-pyrido[4,3-*b*]carbazole-1-carboxamide (25)**

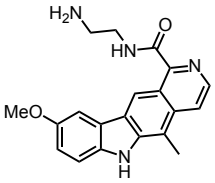

Yield: 20.3 mg, 79%. ^{1}H NMR (700 MHz, DMSO-d_6) δ 11.41 (s, 1H), 9.74 (s, 1H), 9.20 (t, *J* = 5.9 Hz, 1H), 8.47 (d, *J* = 5.9 Hz, 1H), 8.20 (d, *J* = 6.0 Hz, 1H), 7.94 (s, 3H), 7.81 (d, *J* = 2.5 Hz, 1H), 7.50 (d, *J* = 8.6 Hz, 1H), 7.21 (dd, *J* = 2.5, 8.6 Hz, 1H), 3.92 (s, 3H), 3.70 (q, *J* = 6.2 Hz, 2H), 3.13 (h, *J* = 6.2 Hz, 2H), 2.87 (s, 3H). ^{13}C NMR (176 MHz, DMSO-d_6) δ 167.45, 154.04, 151.09, 141.99, 137.86, 137.82, 133.95, 126.62, 123.32, 120.27, 119.57, 117.73, 116.86, 112.38, 111.46, 104.51, 56.13, 39.16, 37.43, 12.93. HR-MS (ESI) calcd. for $C_{20}H_{21}N_4O_2^+$ $[M+H]^+$: 349.1659; found: 349.1653.

***N*-(2-(dimethylamino)ethyl)-9-methoxy-5,6-dimethyl-6*H*-pyrido[4,3-*b*]carbazole-1-carboxamide (26)**

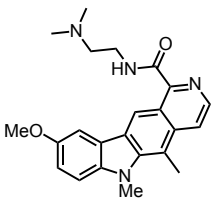

Compound **20** (48 mg, 0.138 mmol) was dissolved in *N*,*N*-dimethylethylenediamine (300 µL), heated to 120 °C, and stirred for 6 h. The reaction mixture was concentrated *in vacuo,* and the crude product was purified by flash chromatography (1-10% MeOH in DCM, linear gradient) providing **26** (50 mg) in 72% yield. ^{1}H NMR (400 MHz, $CDCl_3$) δ 10.06 (s, 1H), 8.60 (t, *J* = 5.8 Hz, 1H), 8.35 (d, *J* = 6.0 Hz, 1H), 7.93 (d, *J* = 6.0 Hz, 1H), 7.71 (d, *J* = 2.2 Hz, 1H), 7.16 – 7.13 (m, 2H), 3.95 (s, 3H), 3.94 (s, 3H), 3.76 (q, *J* = 6.1 Hz, 2H), 2.93 (s, 3H), 2.80 (t, *J* = 6.1 Hz, 2H), 2.47 (s, 6H). ^{13}C NMR (101 MHz, $CDCl_3$) δ 167.54, 154.28, 148.87, 141.94, 139.83, 138.45, 135.63, 127.64, 123.49, 121.40, 119.30, 117.24, 117.02, 110.79, 109.47, 103.97, 58.17, 56.27, 45.22, 36.98, 33.79, 14.09. HR-MS (ESI) calcd. for $C_{23}H_{27}N_4O_2^+$ $[M+H]^+$: 391.2129; found: 391.2130.

_N_-(2-(dimethylamino)ethyl)-9-methoxy-5-methyl-6_H_-pyrido[4,3-_b_]carbazole-1-carboxamide (27)

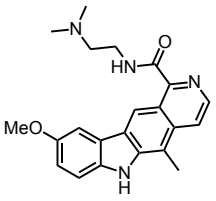

Yield: 7.8 mg, 84%. ^{1}H NMR (400 MHz, CD_3OD) δ 9.25 (s, 1H), 8.37 (d, *J* = 6.5 Hz, 1H), 8.30 (d, *J* = 6.5 Hz, 1H), 7.79 (d, *J* = 2.5 Hz, 1H), 7.47 (d, *J* = 8.8 Hz, 1H), 7.22 (dd, *J* = 2.5, 8.8 Hz, 1H), 4.01 (t, *J* = 5.8 Hz, 2H), 3.56 (t, *J* = 5.8 Hz, 2H), 3.08 (s, 6H), 2.86 (s, 3H). ^{13}C NMR (176 MHz, CD_3OD) δ 166.41, 154.65, 150.34, 143.49, 137.71, 134.08, 132.84, 127.99, 122.82, 119.54, 119.54, 118.82, 117.56, 116.66, 111.63, 111.55, 104.18, 56.69, 55.05, 42.36, 34.77, 10.96. HR-MS (ESI) calcd. for $C_{22}H_{25}N_4O_2^+$ $[M+H]^+$: 377.1972; found: 377.1984.

(*R*)-*N*-(1-(dimethylamino)propan-2-yl)-9-hydroxy-5,6-dimethyl-6*H*-pyrido[4,3-*b*]carbazole-1-carboxamide (28)

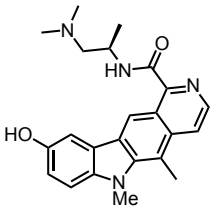

A solution of **29** (14 mg, 0.028 mmol, 1.0 eq) in DCM (1.2 mL) was cooled to -70 °C, and BBr_3 (1 M in DCM, 280 µL, 0.28 mmol, 10 eq) was added. The reaction mixture was allowed to come to room temperature over 5 h with stirring, which was continued for an additional 12 h after reaching room temperature. The reaction was quenched by pouring into ice-water (ca. 5 mL) and subsequent basification with NEt_3. After stirring for 3 h at room temperature, the phases were separated, and the product was extracted with DCM (3×10 mL). The combined organic extracts were dried over Na_2SO_4, filtered, and the solvent was removed under reduced pressure. The crude product was purified by preparative HPLC (linear gradient 10-100% MeCN/MeOH = 1:1, 0.1% TFA, 10 min)) providing **28** (7.7 mg) in 55% yield. ^{1}H NMR (400 MHz, CD_3OD) δ 9.17 (s, 1H), 8.39 (m, 1H), 8.31 (m, 1H), 7.60 (d, *J* = 2.3 Hz, 1H), 7.38 (d, *J* = 8.7 Hz, 1H), 7.14 (dd, *J* = 8.7, 2.4 Hz, 1H), 4.91 (m, 1H, *overlapped with water peak*), 4.15 (s, 3H), 3.51 – 3.34 (2H), 3.22-2.98 (9H), 1.45 (d, *J* = 6.7 Hz, 3H). ^{13}C-NMR (150 MHz, CD_3OD) δ 167.8, 153.3, 151.9, 144.7, 140.7, 136.7, 135.7, 129.8, 124.0, 120.9, 120.5, 118.8, 117.4, 113.4, 111.2, 107.3, 63.3, 45.7 (br), 42.9, 42.7 (br), 34.1, 18.8, 14.1 HR-MS (ESI) calcd. for $C_{23}H_{27}N_4O_2^+$ $[M+H]^+$: 391.2129; found: 391.2130

(*R*)-*N*-(1-(dimethylamino)propan-2-yl)-9-methoxy-5,6-dimethyl-6*H*-pyrido[4,3-*b*]carbazole-1-carboxamide (29)

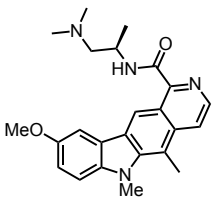

To a solution of **20** (20 mg, 0.057 mmol, 1.0 eq) in EtOH (1.5 mL) was added NaOH (171 µL, 0.171 mmol, 3.0 eq), and the mixture was refluxed for 90 min at 83 °C. After neutralization with HCl (1 M), the reaction mixture was concentrated *in vacuo* and lyophilized to give the corresponding acid in quantitative yield. The acid (10 mg, 0.022 mmol, 1.0 eq) was dissolved in DMF (0.5 mL), and EDC (6.3 mg, 0.033 mmol, 1.5 eq), HOBt (4.4 mg, 0.033 mmol, 1.5 eq) and DIPEA (11 µL, 0.066 mmol, 3.0 eq) were added. The mixture was stirred for 5 min at room temperature before (*R*)-N^1,N^1-dimethylpropane-1,2-diamine (4.5 mg, 0.044 mmol, 2.0 eq) was added. After stirring for 20 h at room temperature, the solvent was evaporated and the product was purified by reversed phase flash chromatography (0-100% MeOH in H_2O, 0.1% TFA, linear gradient) providing **29** (7.2 mg) in 63% yield. ^{1}H NMR (700 MHz, CD_3OD) δ 9.05 (s, 1H), 8.31 (d, *J* = 6.0 Hz, 1H), 8.23 (d, *J* = 6.1 Hz, 1H), 7.64 (s, 1H), 7.32 (dd, *J* = 1.9, 8.8 Hz, 1H), 7.22 – 7.13 (m, 1H), 4.00 (s, 3H), 3.93 (s, 3H), 3.54 – 3.48 (m, 1H), 3.45 – 3.39 (m, 1H), 3.29 – 3.02 (m, 7H), 2.96 (s, 3H), 1.50 (d, *J* = 6.8 Hz, 2H). ^{13}C NMR (176 MHz, CD_3OD) δ 164.98, 154.84, 149.66, 143.20, 139.43, 135.16, 132.15, 128.38, 121.92, 119.65, 118.50, 117.23, 116.48, 112.16, 109.86, 103.80, 61.77, 55.03, 41.60, 32.53, 17.40, 12.57. HR-MS (ESI) calcd. for $C_{24}H_{29}N_4O_2^+$ $[M+H]^+$: 405.2285; found: 405.2277.

(*R*)-*N*-(1-(dimethylamino)propan-2-yl)-9-methoxy-5-methyl-6*H*-pyrido[4,3-*b*]carbazole-1-carboxamide (30)

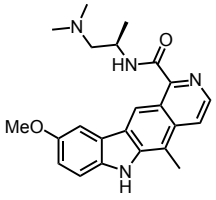

To a solution of **19** (25 mg, 0.075 mmol, 1.0 eq) in EtOH (1.5 mL) was added NaOH (225 µL, 0.171 mmol, 3.0 eq), and the mixture was refluxed for 90 min at 83 °C. After neutralization with HCl (1 M), the reaction mixture was concentrated *in vacuo* and lyophilized to give the corresponding acid in quantitative yield. The acid (21.5 mg, 0.038 mmol, 1.0 eq) was dissolved in DMF (0.5 mL), and EDC (11 mg, 0.056 mmol, 1.5 eq), HOBt (7.6 mg, 0.056 mmol, 1.5 eq) and DIPEA (19 µL, 0.113 mmol, 3.0 eq) were added. The mixture was stirred for 5 min at room temperature before (*R*)-N^1,N^1-dimethylpropane-1,2-diamine (7.7 mg, 0.075 mmol, 2.0 eq) was added. After stirring for 14 h at room temperature, the solvent was evaporated, and the product was purified by reversed phase flash chromatography (0-100% MeOH in H_2O, 0.1% TFA, linear gradient) providing **30** (15 mg) in 79% yield. ^{1}H NMR (700 MHz, CD_3OD) δ 9.17 (s, 1H), 8.35 (d, *J* = 7.1 Hz, 1H), 8.29 (d, *J* = 6.7 Hz, 1H), 7.76 (dd, *J* = 3.8, 7.3 Hz, 1H), 7.51 – 7.43 (m, 1H), 7.23 (d, *J* = 8.6 Hz, 1H), 3.95 (s, 3H), 3.54 – 3.48 (m, 1H), 3.45 – 3.38 (m, 1H), 3.12 (s, 7H), 3.03 – 2.90 (m, 1H), 2.89 – 2.78 (m, 3H), 1.51 (d, *J* = 6.6 Hz, 2H). ^{13}C NMR (176 MHz, CD_3OD) δ 165.24, 154.69, 150.29, 143.72, 137.65, 134.06, 131.87, 128.07, 122.66, 119.60, 118.51, 117.64, 116.74, 111.68, 104.20, 61.87, 55.04, 41.64, 17.35, 10.94. HR-MS (ESI) calcd. for $C_{23}H_{27}N_4O_2^+$ $[M+H]^+$: 391.2129; found: 391.2121.

Compound 2

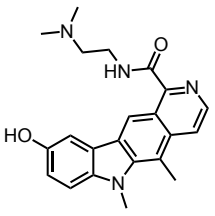

Compound **2** was synthesized by the aminolysis method mentioned above. ^{1}H NMR (700 MHz, CD_3OD) δ 9.12 (s, 1H), 8.33 (d, *J* = 6.4 Hz, 1H), 8.25 (d, *J* = 6.4 Hz, 1H), 7.55 (d, *J* = 2.2 Hz, 1H), 7.30 (d, *J* = 8.7 Hz, 1H), 7.12 (dd, *J* = 8.6, 2.2 Hz, 1H), 4.05 (s, 3H), 4.00 (t, *J* = 5.8 Hz, 2H), 3.55

(t, *J* = 5.8 Hz, 2H), 3.08 (s, 6H), 3.03 (s, 3H). ^{13}C NMR (176 MHz, CD_3OD) δ 167.8, 153.3., 151.1, 144.7, 140.5, 136.7, 134.9, 129.8, 123.9, 121.0, 120.3, 118.8, 117.7, 113.3, 111.1, 107.4, 58.1, 43.8, 36.2, 34.1, 14.1 HRMS (ESI) calcd. for $C_{22}H_{25}N_4O_2^+$ $[M+H]^+$: 377.1972; found: 377.1986.

Compound 1

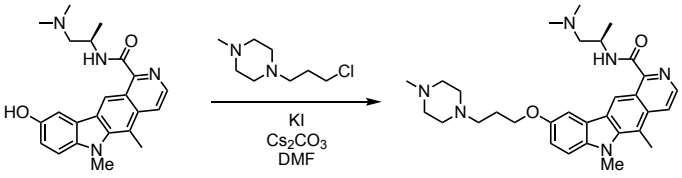

To a solution of phenol **28** (195 mg, 0.5 mmol) in DMF (6 mL) was added Cs_2CO_3 (489 mg, 1.5 mmol), KI (83 g, 0.5 mmol), and alkyl chloride (150 mg, 0.6 mmol). The mixture was stirred at 70 ˚C overnight. The crude mixture was diluted 10-fold by addition of 54 mL of H_2O and acidified by the addition of TFA. The product was purified by HPLC (0-40% MeCN/H_2O in 60 min, 0.1% TFA) to give **1** as a red solid (58 mg, 58 μmol, 12%). ^{1}H NMR (600 MHz, DMSO-d_6): δ = 9.82 (s, 1H), 9.44 (br, 1H), 9.16 (d, *J* = 9.1 Hz, 1H), 8.50 (d, *J* = 6.1 Hz, 1H), 8.30 (m, 1H), 7.81 (d, *J* = 2.4 Hz, 1H), 7.62 (d, *J* = 8.9 Hz, 1H), 7.27 (dd, *J* = 8.9, 2.5 Hz, 1H), 4.63 (m, 1H), 4.28-4.14 (5H), 3.94-2.99 (15H), 2.99-2.76 (9H), 2.16 (m, 2H), 1.32 (d, *J* = 6.7 Hz, 3H); ^{13}C NMR (150 MHz, DMSO-d_6): δ = 166.6, 158.5 (q, *J* = 33.7 Hz), 152.9, 150.1, 141.5, 139.7, 138.3, 134.9, 126.5, 122.3, 120.3, 119.3, 117.4, 116.4, 111.9, 110.5, 105.0, 65.8, 60.5, 53.2, 50.4, 48.6, 43.9, 42.1, 40.8, 33.6, 24.4, 18.8, 13.6; HR-MS (MALDI): Calcd. for $C_{31}H_{43}N_6O_2^+$ $[M+H]^+$: 531.3442; found: 531.3419.

Compound 35: intermediate i1b

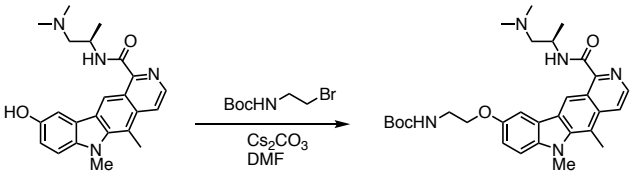

To a solution of phenol **28** (20 mg, 51.2 μmol) and Cs_2CO_3 (33.4 mg, 102 μmol) in DMF (500 μL) was added alkyl bromide (13.8 mg, 61.4 μmol). The mixture was stirred at room temperature overnight. Cs_2CO_3 (33.4 mg, 102 μmol) and alkyl bromide (27.6 mg, 123 μmol) were added to the solution, and the mixture was stirred at room temperature for 4 h. The consumption of phenol was confirmed by MALDI MS, and the product was extracted with AcOEt and washed with water. After washing of organic layer with brine, the solution was dried with Na_2SO_4. The crude mixture was purified by silica gel column chromatography (DCM:MeOH=100:0 to 70:30, 1% Et_3N) to give **i1** as a yellow solid (22.8 mg, 42.7 μmol, 83%). ^{1}H NMR (600 MHz, CD_3OD): δ = 9.31 (s, 1H), 8.30 (d, *J* = 6.1 Hz, 1H), 7.98 (d, *J* = 6.0 Hz, 1H), 7.58 (m, 1H), 7.22 (d, *J* = 8.7 Hz, 1H), 7.13 (dd, *J* = 8.7, 2.3 Hz, 1H), 4.47 (m, 1H), 4.09 (t, *J* = 5.5 Hz, 2H), 3.92 (s, 3H), 3.51 (t, *J* = 5.7 Hz, 2H), 2.89 (s, 3H), 2.68 (dd, *J* = 12.5, 8.2 Hz, 1H), 2.45 (dd, *J* = 12.5, 6.0 Hz, 1H), 2.39 (s, 6H), 1.48 (s, 9H), 1.39 (d, *J* = 6.6 Hz, 3H); ^{13}C NMR (150 MHz, CD_3OD): δ = 169.3, 158.6, 154.7, 153.3, 143.1, 141.2, 139.4, 136.3, 128.4, 124.1, 121.5, 119.7, 118.3, 117.0, 112.5, 110.7, 106.0, 80.2, 69.0, 65.8, 46.1, 44.9, 41.2, 33.9, 28.8, 19.5, 13.9; HR-MS (MALDI): Calcd. for $C_{30}H_{40}N_5O_4^+$ $[M+H]^+$: 534.3075; found: 534.3072.

Compound 35: intermediate i2b

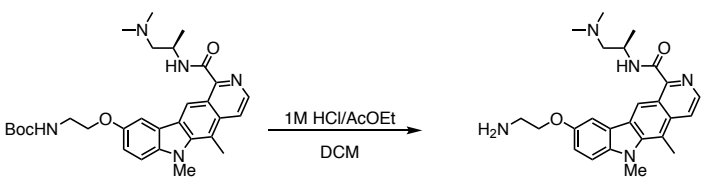

A solution of **i1b** (15.8 mg, 29.6 μmol) and 1 M HCl/AcOEt (2 mL) in DCM (4 mL) was stirred at 45 ˚C for 1 h. The solvent was evaporated to give **i2** as an orange solid (15.1 mg, 27.8 μmol, 94%). ^{1}H NMR (600 MHz, CD_3OD): δ = 9.11 (s, 1H), 8.45 (m, 1H), 8.31 (m, 1H), 7.95 (m, 1H), 7.62 (d, *J* = 8.9 Hz, 1H), 7.43 (dd, *J* = 8.8, 2.1 Hz, 1H), 5.01 (m, 1H), 4.52-4.35 (2H), 4.26 (s, 3H), 3.58-3.46 (4H), 3.20 (brs, 3H), 3.13 (s, 3H), 3.07 (brs, 3H), 1.55 (d, *J* = 6.3 Hz, 3H); ^{13}C NMR (150 MHz, CD_3OD): δ = 163.4, 155.1, 149.8, 146.3, 141.6, 137.3, 130.8, 128.5, 123.1, 122.0, 120.2, 119.9, 119.0, 114.8, 112.1, 107.0, 66.3, 63.1, 46.1, 43.7, 42.8, 40.6, 34.4, 19.0, 14.2; HR-MS (MALDI): Calcd. for $C_{25}H_{32}N_5O_2^+$ $[M+H]^+$: 434.2551; found: 434.2543.

Compound 35

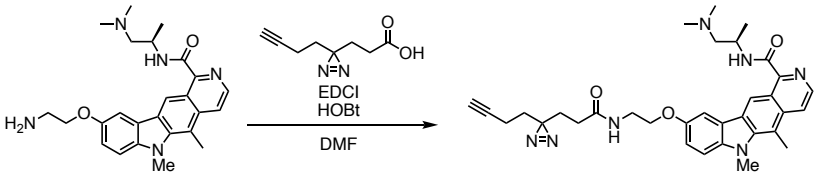

A mixture of carboxylic acid (6.6 mg, 40 μmol), EDCI (7.6 mg, 40 μmol), and HOBt (6.2 mg, 40 μmol) in DMF (0.7 mL) was stirred for 15 min at room temperature. To the solution was added a mixture of i2 (7.2 mg, 13.3 μmol) and DIPEA (23 μL, 133 μmol) in DMF (0.3 mL), and the solution was stirred overnight. The product was purified by HPLC (45-75% MeOH/H_2O in 30 min, 0.1% TFA) to give **35** as a red solid (8.8 mg, 10.8 μmol, 83%). ^{1}H NMR (600 MHz, CD_3OD): δ = 9.22 (s, 1H), 8.39 (br, 1H), 8.29 (br, 1H), 7.78 (d, *J* = 2.4 Hz, 1H), 7.42 (d, *J* = 8.8 Hz, 1H), 7.27 (dd, *J* = 8.8, 2.5 Hz, 1H), 4.94-4.89 (m, 1H, *overlapped with water peak*), 4.20 (t, *J* = 5.4 Hz, 2H), 4.13 (s, 3H), 3.64 (t, *J* = 5.4 Hz, 2H), 3.47 (m, 1H), 3.39 (m, 1H), 3.19-2.99 (9H), 2.25 (t, *J* = 2.7 Hz, 1H), 2.10 (dd, *J* = 8.1, 7.1 Hz, 2H), 1.97 (td, *J* = 7.5, 2.7 Hz, 2H), 1.75 (dd, *J* = 8.2, 7.0 Hz, 2H), 1.59 (t, *J* = 7.5 Hz, 2H), 1.46 (d, *J* = 6.7 Hz, 3H); ^{13}C NMR (150 MHz, CD_3OD): δ = 174.8, 168.0, 155.2, 152.2, 144.5, 141.4, 136.7, 136.1, 129.6, 123.8, 120.9, 120.7, 119.3, 117.6, 113.6, 111.3,

106.4, 83.6, 70.4, 68.5, 63.3, 45.8, 42.8, 42.7, 40.4, 34.1, 33.3, 31.0, 30.0, 28.9, 18.9, 14.1, 13.8; HR-MS (MALDI): Calcd. for $C_{33}H_{40}N_7O_3^+$ $[M+H]^+$: 582.3187; found: 582.3179.

Compound 36

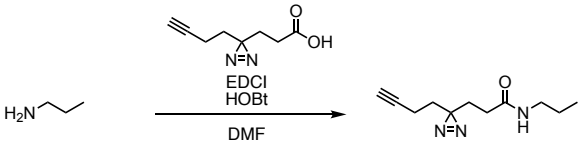

HR-MS (ESI): Calcd. for $C_{12}H_{18}N_3O_3^-$ $[M+HCOO]^-$: 252.1354; found: 252.1347.

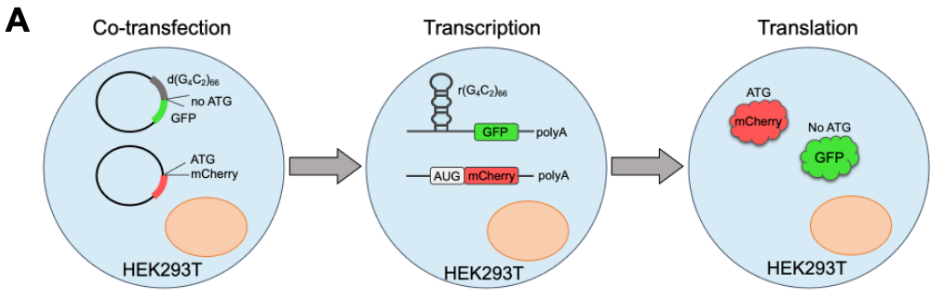
A
Co-transfection
Transcription
Translation
d(G4C2)66
no ATG
GFP
ATG
mCherry
HEK293T
r(G4C2)66
GFP
polyA
AUG
mCherry
polyA
HEK293T
ATG
mCherry
No ATG
GFP
HEK293T

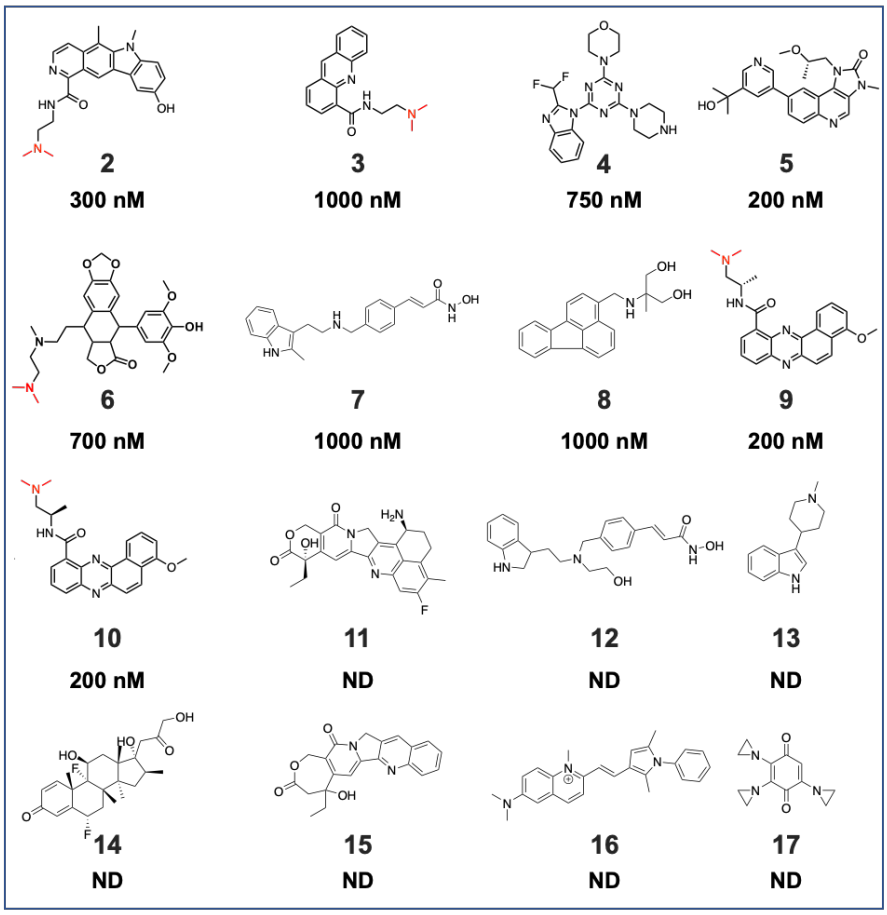
B
2
300 nM
3
1000 nM
4
750 nM
5
200 nM
6
700 nM
7
1000 nM
8
1000 nM
9
200 nM
10
200 nM
11
ND
12
ND
13
ND
14
ND
15
ND
16
ND
17
ND

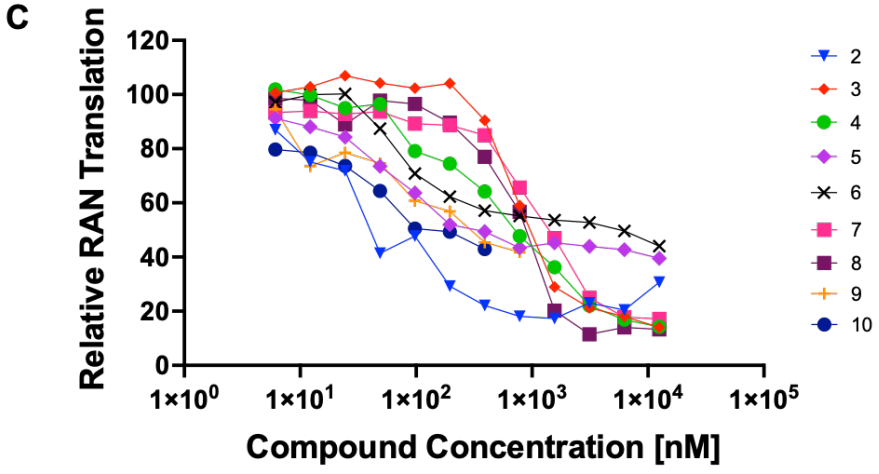
C
Relative RAN Translation
120
100
80
60
40
20
0
1×10^0
1×10^1
1×10^2
1×10^3
1×10^4
1×10^5
Compound Concentration [nM]
2
3
4
5
6
7
8
9
10

Fig. S1. Screen of the ReFRAME small molecule library (14) for inhibitiors of RAN translation in a cellular model of c9ALS/FTD. (A) Schematic of RAN translation assay in HEK293T co-transfected with *$(G_4C_2)_{66}$-No ATG-GFP* (disease; RAN translation) or *SV40-mCherry* (control; canonical translation). **(B)** Structures of small molecule hits from the primary screen of ReFRAME. Compounds **2** – **10** exhibited a dose-response in secondary validation activities (while **11** – **17** did not), and their approximate IC_{50} values are provided below the compound number. ND indicates no determination was possible. The first nine compounds shown possess common structural features, for example all share a flat aromatic core-scaffold capable of inducing π-π stacking interactions, and five compounds have a dimethylamine substituted side chain (highlighted in red; **2, 3, 6, 9,** and **10**). **(C)** Dose-responses of hit compounds for inhibiting RAN translation, as assessed in HEK293T cells dually transfected with *$(G_4C_2)_{66}$-No ATG-GFP* and *SV40-mCherry*.

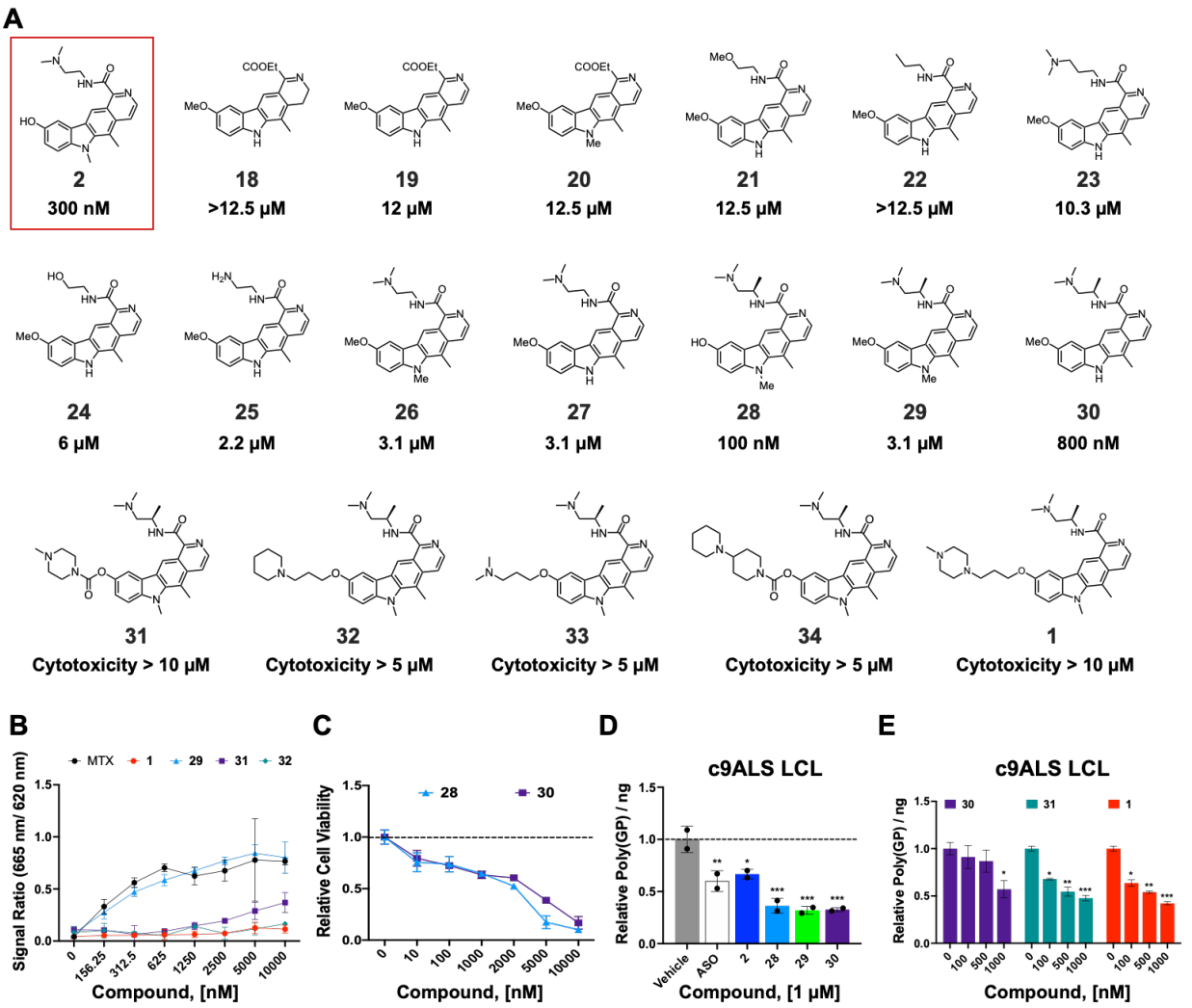

Fig. S2. SAR optimization of r(G$_4$C$_2$)^{exp}-targeting small molecule lead 2. (A) Chemical structures of **2**-derivatives (n = 19) to derive SAR and the corresponding IC$_{50}$s, as determined by RAN translation assay in HEK293T cells. **(B)** Compound-induced DNA damage in HEK239T cells, as determined by measuring γ-H2AX immunofluorescence (n = 3). MTX (mitoxantrone) was used as a positive control. **(C)** Toxicity of **28** and **30** in HEK293T cells, as determined by CellTiter Fluor. **(D)** Compounds **2**, **28** – **30** (1 μM) reduce poly(GP) levels in a single patient-derived LCL (n = 3). **(E)** Compounds **1** and **31** reduced poly(GP) levels in c9ALS patient-derived lymphoblastoid cells in dose-dependent fashion and more potently than first-generation compound **30**. Poly(GP) levels were measured using an electroluminescent sandwich assay (n = 3 in one patient-derived LCL). *P < 0.05, **P < 0.01, ***P < 0.001 as determined by a One-way ANOVA test with multiple comparison (Panel D and E). Error bars indicate SD.

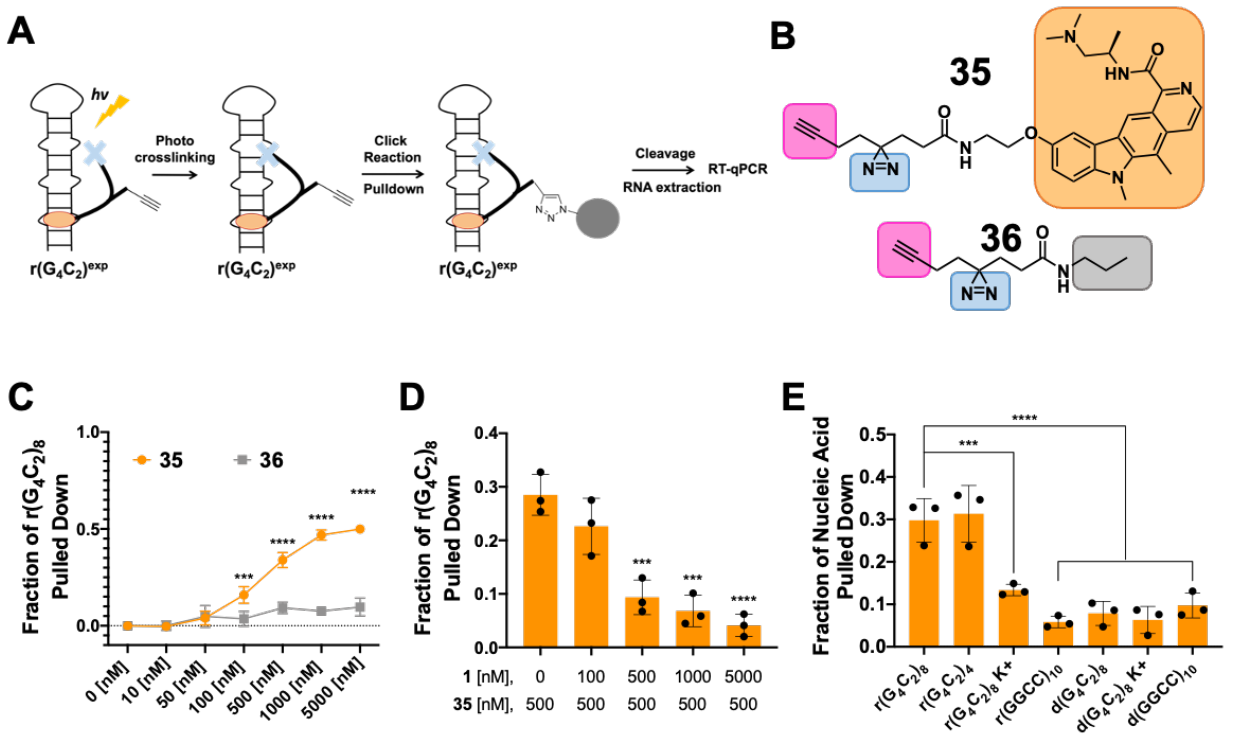

Fig. S3. Small molecules targeting r(G4C2)^{exp} directly engage the target *in vitro* as determined by Chemical Cross-Linking and Isolation by Pull-down (Chem-CLIP). **(A)** Schematic of Chem-CLIP. **(B)** Structures of Chem-CLIP probe **35** and control Chem-CLIP probe **36**, which lacks the RNA-binding module. **(C)** Plot of fraction of r(G4C2)8 pulled down as a function of **35** or **36** concentration (n = 3 technical replicates). Statistical significance was calculated for the difference of the fraction of RNA pulled down for **35** *vs*. **36**. **(D)** Plot of fraction of r(G4C2)8 pulled down by **35** (500 nM), as a function of the concentration of **1**, or a Competitive (C-)Chem-CLIP experiment (n = 3 technical replicates). **(E)** Plot of fraction of r(G4C2)8, r(G4C2)4 [forms the same 1×1 GG loops as r(G4C2)8], r(G4C2)8 + K^+ (predominantly quadruplex form), r(G2C2)10, d(G4C2)8, d(G4C2)8 + K^+, and d(G2C2)10 pulled down by **35**. ***P<0.001, and ****P < 0.0001, as determined by a one-way ANOVA test (Panels C-D). Error bars indicate SD.

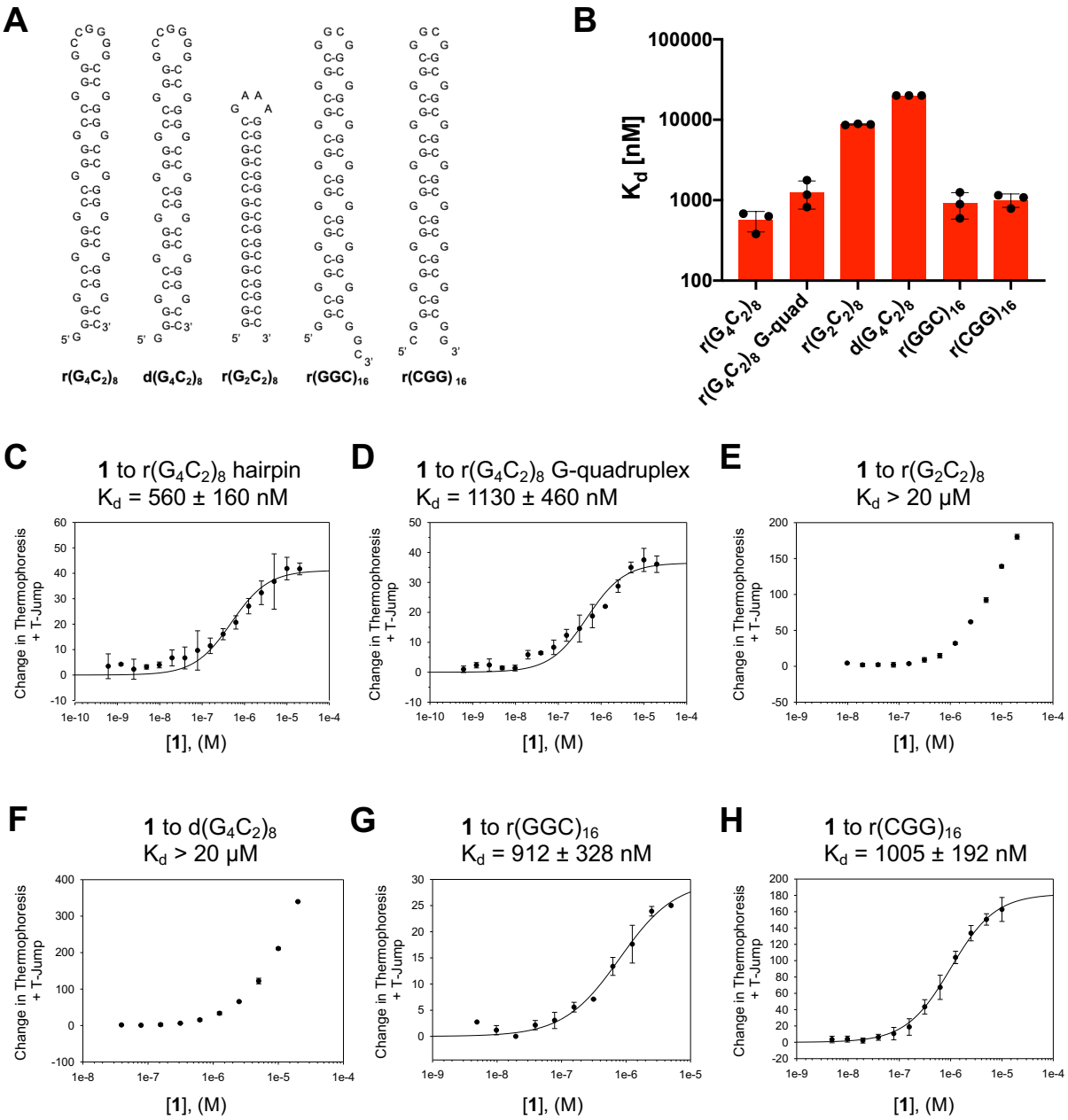

Fig. S4. Compound 1 selectively binds the target $r(G_4C_2)_8$ *in vitro* as determined by affinity measurements. **(A)** Secondary structures of the oligonucleotides used in binding selectivity studies. **(B)** Binding of **1** to $r(G_4C_2)_8$, and several control sequences reported as K_ds as measured by microscale thermophoresis (MST; n = 3). **(C)** Representative binding curve of **1** to $r(G_4C_2)_8$ (n = 3). **(D)** Representative binding curve of **1** to $r(G_4C_2)_8$ in the presence of K^+ such that the equilibrium between hairpin and G-quadruplex forms are shifted towards the G-quadruplex (15) (n = 3). **(E)** Representative binding curve of **1** to $r(G_2C_2)_8$ (n = 3). **(F)** Representative binding curve of **1** to $d(G_4C_2)_8$ (n = 3). **(G)** Representative binding curve of **1** to $r(GGC)_{16}$ (n = 3). **(H)** Representative binding curve of **1** to $r(CGG)_{16}$ (n = 3). Error bars indicate SD.

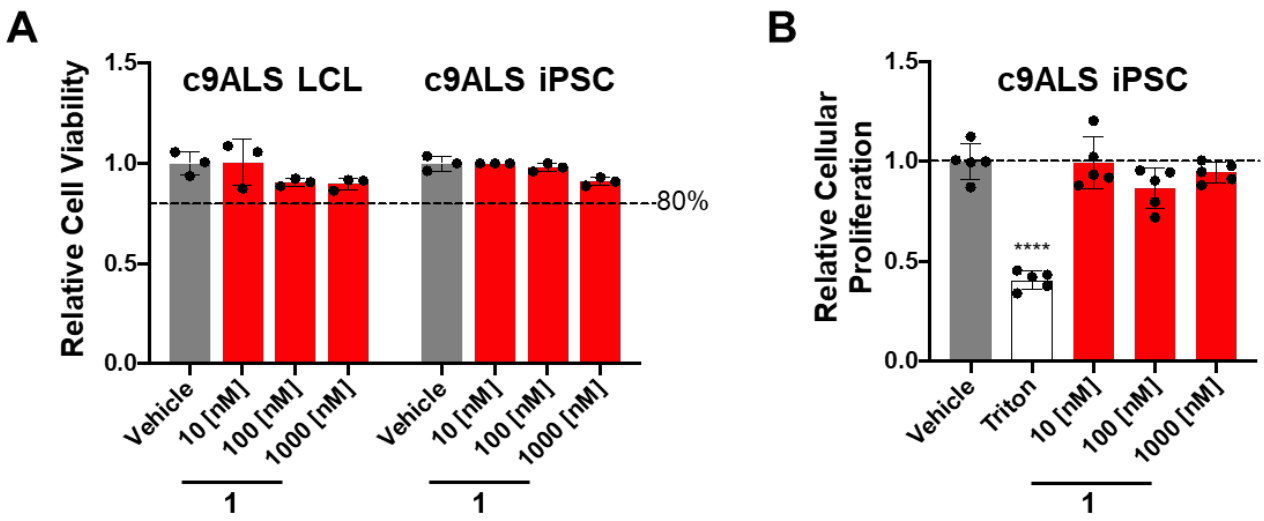

Fig. S5. Compound 1 has no effect on cellular viability or proliferation in patient-derived cell lines. **(A)** Cytotoxicity of **1**, as determined using CellTiter Fluor (n = 1 LCL; 3 replicates) or AlamarBlue (n = 1 iPSC line; 3 replicates) after a 4 day treatment period. **(B)** Effects of **1** on cellular proliferation as determined by a Click-IT Edu assay following manufacturers protocol after 4-day treatment in a single c9ALS patient-derived iPSC line (n = 3 replicates). ****P < 0.0001 as determined by a one-way ANOVA test with multiple comparison (Panel B). Error bars indicate SD.

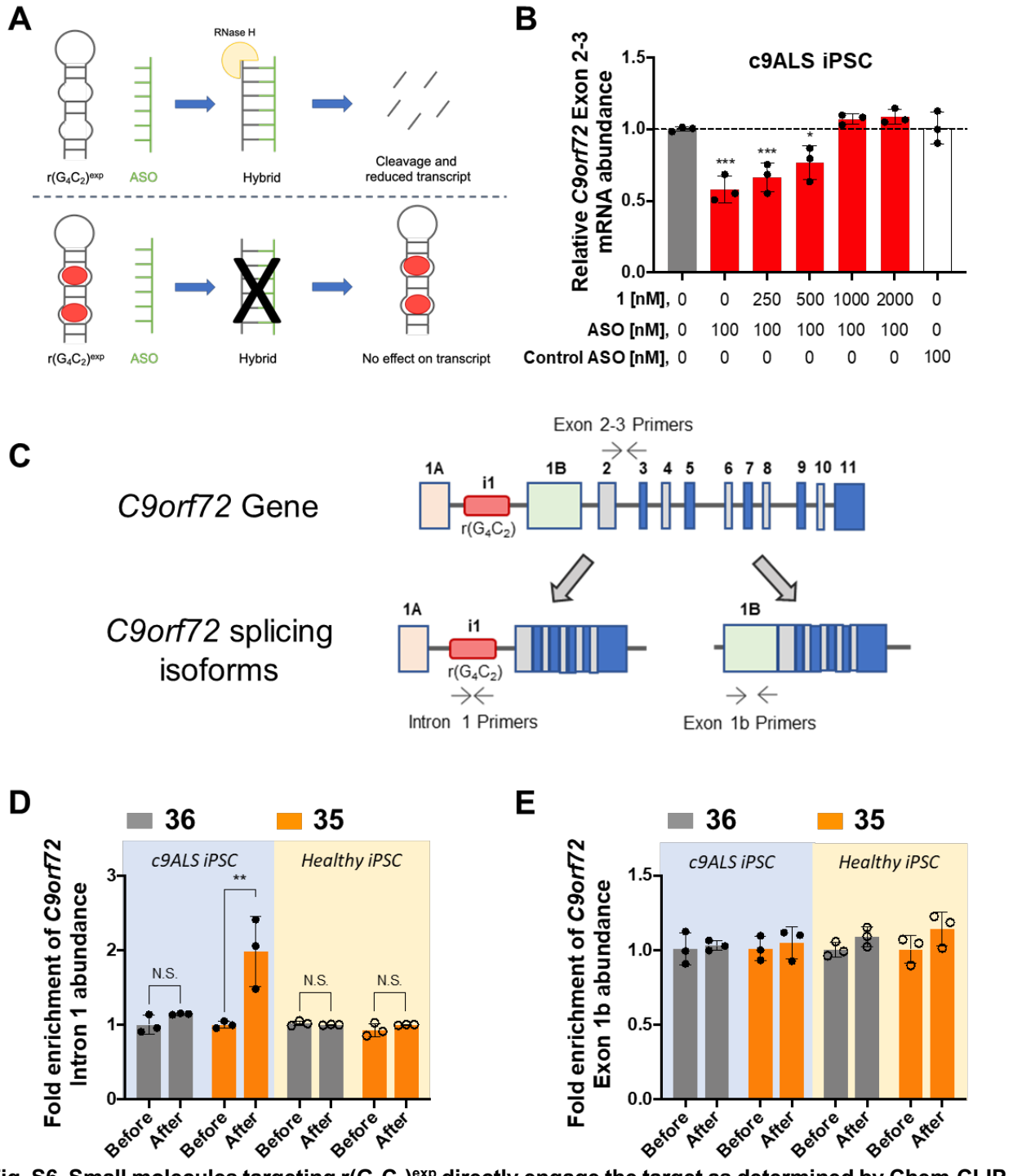

Fig. S6. Small molecules targeting r(G$_4$C$_2$)^{exp} directly engage the target as determined by Chem-CLIP and ASO Bind-Map in c9ALS patient-derived cells. **(A)** Schematic representation of ASO-Bind-Map. **(B)** ASO-Bind-Map target validation of **1**, treated in competition with 100 nM ASO targeting the r(G$_4$C$_2$)^{exp} or a scrambled control ASO in c9ALS patient-derived iPSCs, as determined by RT-qPCR using primers for the *C9orf72* exon 2-3 junction common to all transcripts (n = 3 biological replicates from a single line of patient-derived iPSCs). **(C)** Schematic representation of the transcript variants from *C9orf72* measured. **(D)** Fold-enrichment of *C9orf72* intron 1 in Chem-CLIP studies completed in c9ALS patient-derived iPSCs treated with **35** or **36**. Intron 1 harbors the r(G$_4$C$_2$)$_8$ repeat expansion n = 3 biological replicates from a single line of patient-derived iPSC cell line). **(E)** Fold-enrichment of *C9orf72* exon 1b in Chem-CLIP studies

completed in c9ALS patient-derived iPSCs treated with **35** or **36**. Exon 1b is unique to variants that do not harbor the r$(G_4C_2)_8$ repeat expansion (n = 3 biological replicates from a single line of patient-derived iPSC cell line. *P<0.05, **P<0.01, ***P<0.001, and ****P < 0.0001, as determined by a one-way ANOVA test with multiple comparison (Panel B), or an unpaired t-test with Welch's correction (Panel D). Data are reported as mean ± SD.

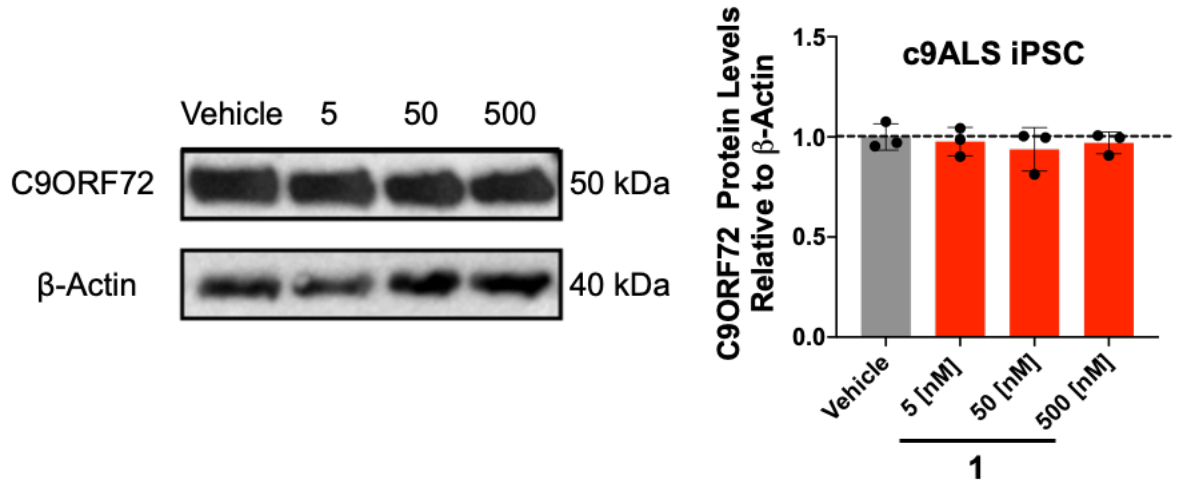

Fig. S7. Compound 1 does not affect C9ORF72 protein levels in patient-derived cells. Relative abundance of WT C9ORF72 protein and β-actin in patient-derived iPSCs treated with vehicle or **1** at 5, 50, and 500 nM, as determined by Western blotting. Left, Representative image of a Western blot; Right, Quantification of native *C9orf72* protein levels, as normalized to levels of β-actin (n = 1 c9ALS iPSC line, 3 replicates). Error bars indicate SD.

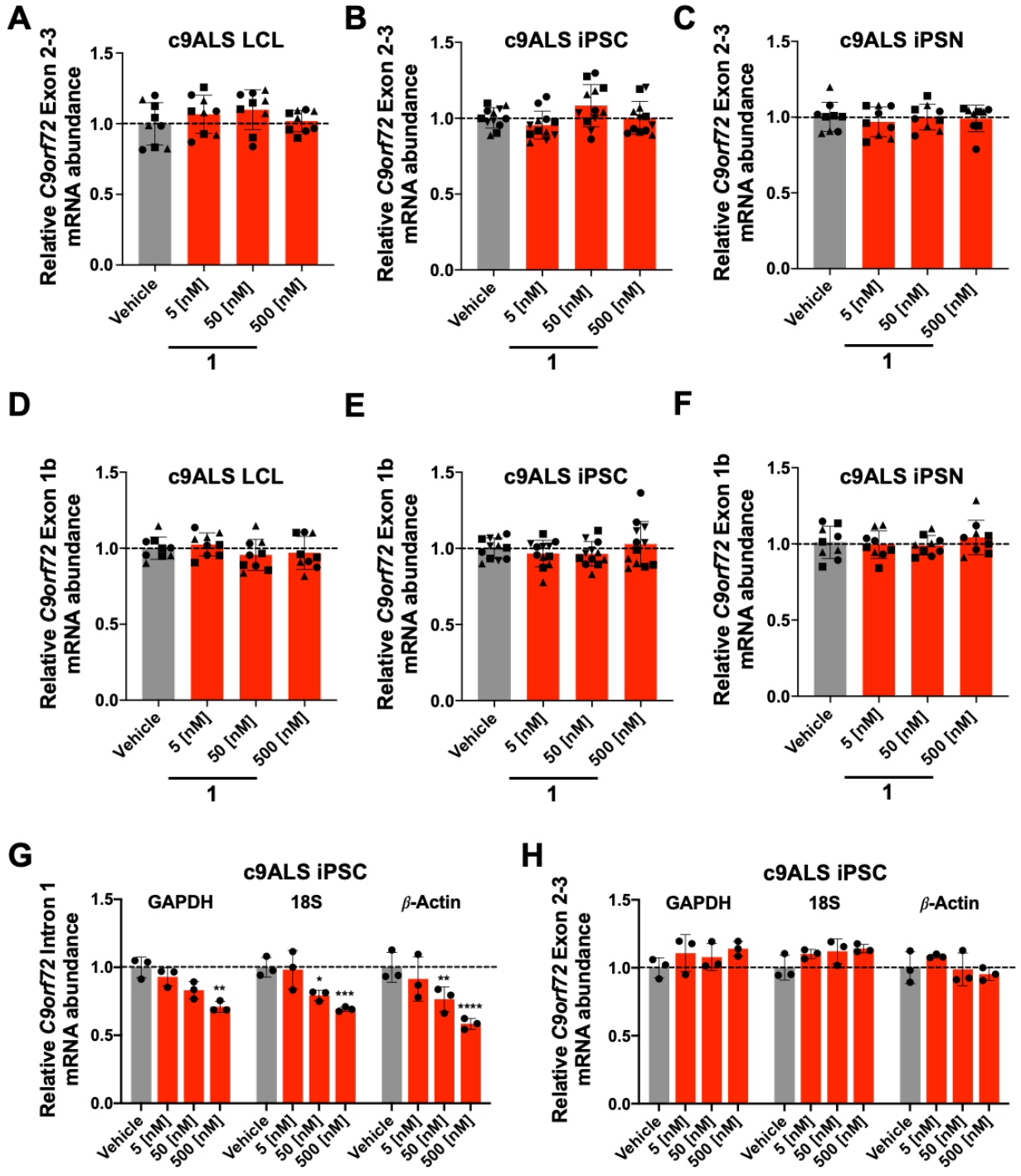

Fig. S8. Compound 1 does not affect total *C9orf72* levels or the levels of variants lacking the repeat expansion. **(A)** Effect of **1** on *C9orf72* exon 2-3 levels, common to all transcripts, in c9ALS patient-derived LCLs, as determined by RT-qPCR with exon 2-3-specific primers (n = 3 c9ALS LCLs; 3 replicates per line). **(B)** Effect of **1** on *C9orf72* exon 2-3 levels in c9ALS patient-derived iPSCs, as determined by RT-qPCR with exon 2-3-specific primers (n = 4 c9ALS iPSC lines; 3 replicates per line). **(C)** Effect of **1** on *C9orf72* exon 2-3 levels in c9ALS patient-derived iPSNs, as determined by RT-qPCR with exon 2-3-specific primers (n = 3 c9ALS iPSN lines; 3 replicates per line). **(D)** Effect of **1** on *C9orf72* exon 1b levels, which does not

possess the r(G_4C_2)^{exp}, in c9ALS patient-derived LCLs, as determined by RT-qPCR with exon 1b-specific primers (n = 3 c9ALS LCLs; 3 replicates per line). **(E)** Effect of **1** on *C9orf72* exon 1b levels in c9ALS patient-derived iPSCs, as determined by RT-qPCR with exon 1b-specific primers (n = 4 c9ALS iPSC lines; 3 replicates per line). **(F)** Effect of **1** on *C9orf72* exon 1b levels in c9ALS patient-derived iPSNs, as determined by RT-qPCR with exon 1b-specific primers (n = 3 c9ALS iPSN lines; 3 replicates per line). **(G)** Effect of **1** on *C9orf72* intron 1 levels, which harbors r(G_4C_2)^{exp}, in patient-derived iPSC cells as determined by RT-qPCR with intron 1-specific primers relative to *GAPDH*, *18S*, and *β-actin* housekeeping genes (n = 1 c9ALS iPSC line; n = 3 replicates). **(H)** Effect of **1** on *C9orf72* exon 2-3 levels in patient-derived iPSCs, as determined by RT-qPCR with exon 2-3-specific primers relative to *GAPDH*, *18S*, and *β-actin* housekeeping genes (n = 1 c9ALS iPSC line; n = 3 replicates). RNA quantification was measured relative to *GAPDH* in Panels A-F. Vehicle indicates 0.1% (v/v) DMSO. *P < 0.05, **P < 0.01, ***P < 0.001 , ****P < 0.0001, as determined by a one way ANOVA with multiple comparisons (Panel G). Error bars indicate SD.

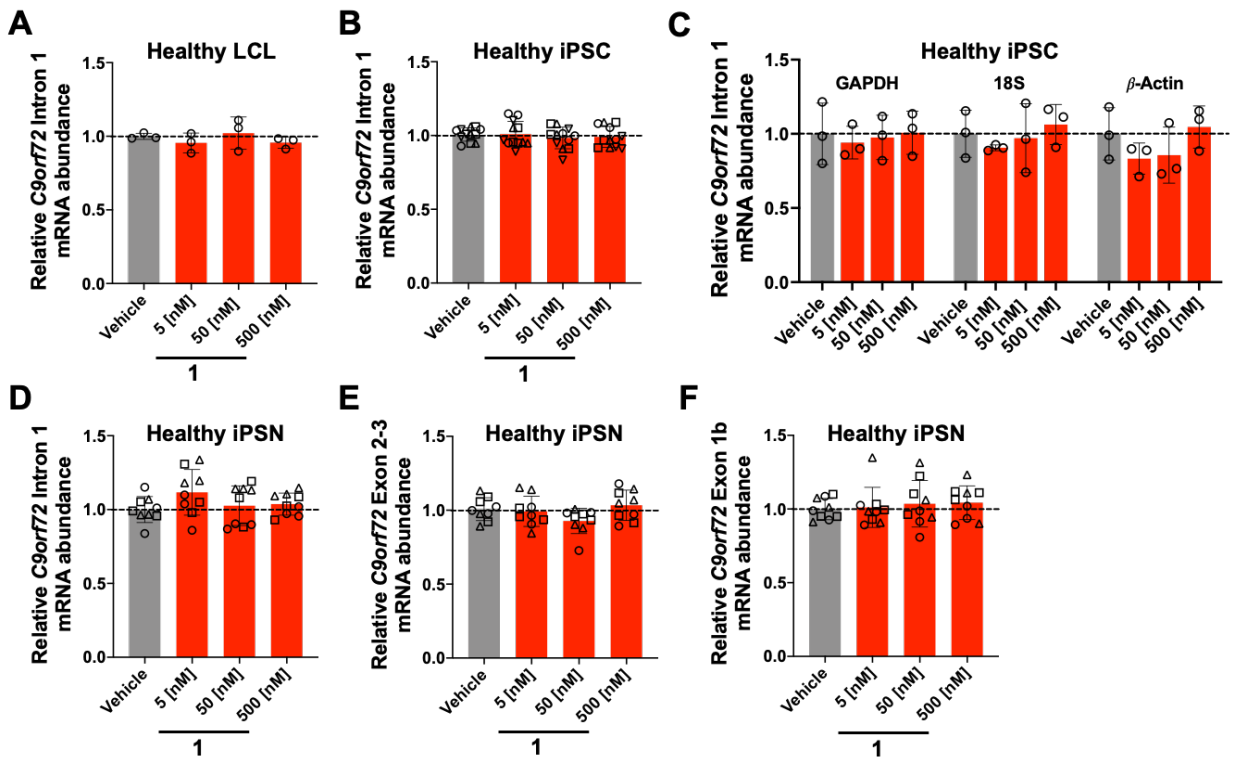

Fig. S9. Compound 1 does not affect *C9orf72* intron 1 levels or total *C9orf72* mRNA levels in cells from healthy donors. **(A)** Effect of **1** on *C9orf72* intron 1 levels in healthy patient-derived LCLs, as determined by RT-qPCR with intron 1-specific primers (n = 1 healthy LCL; 3 replicates). **(B)** Effect of **1** on *C9orf72* intron 1 levels in iPSCs derived from healthy donors, as determined by RT-qPCR with intron 1-specific primers (n = 4 healthy iPSC lines; 3 replicates per line). **(C)** Effect of **1** on *C9orf72* intron 1 levels, which harbors $r(G_4C_2)^{exp}$, in iPSCs from healthy donors, as determined by RT-qPCR with intron 1-specific primers relative to *GAPDH*, *18S*, and *β-actin* housekeeping genes (n = 1 healthy iPSC line; n = 3 replicates). **(D)** Effect of **1** on *C9orf72* intron 1 levels, which harbors $r(G_4C_2)^{exp}$, in iPSNs derived from healthy donors, as determined by RT-qPCR with exon 1-specific primers (n = 3 iPSN lines; 3 replicates per line). **(E)** Effect of **1** on *C9orf72* exon 2-3 levels, common to all transcripts in iPSNs from healthy donors, as determined by RT-qPCR with exon 2-3-specific primers (n = 3 iPSN lines; 3 replicates per line). **(F)** Effect of **1** on *C9orf72* transcripts with exon 1b, which do not possess the $r(G_4C_2)^{exp}$, in iPSNs from healthy donors, as determined by RT-qPCR with exon 1b-specific primers (n = 3 iPSN lines; 3 replicates per line). RNA quantification was measured relative to *GAPDH* in Panels A, B, D-F. Vehicle indicates 0.1% (v/v) DMSO. Error bars indicate SD.

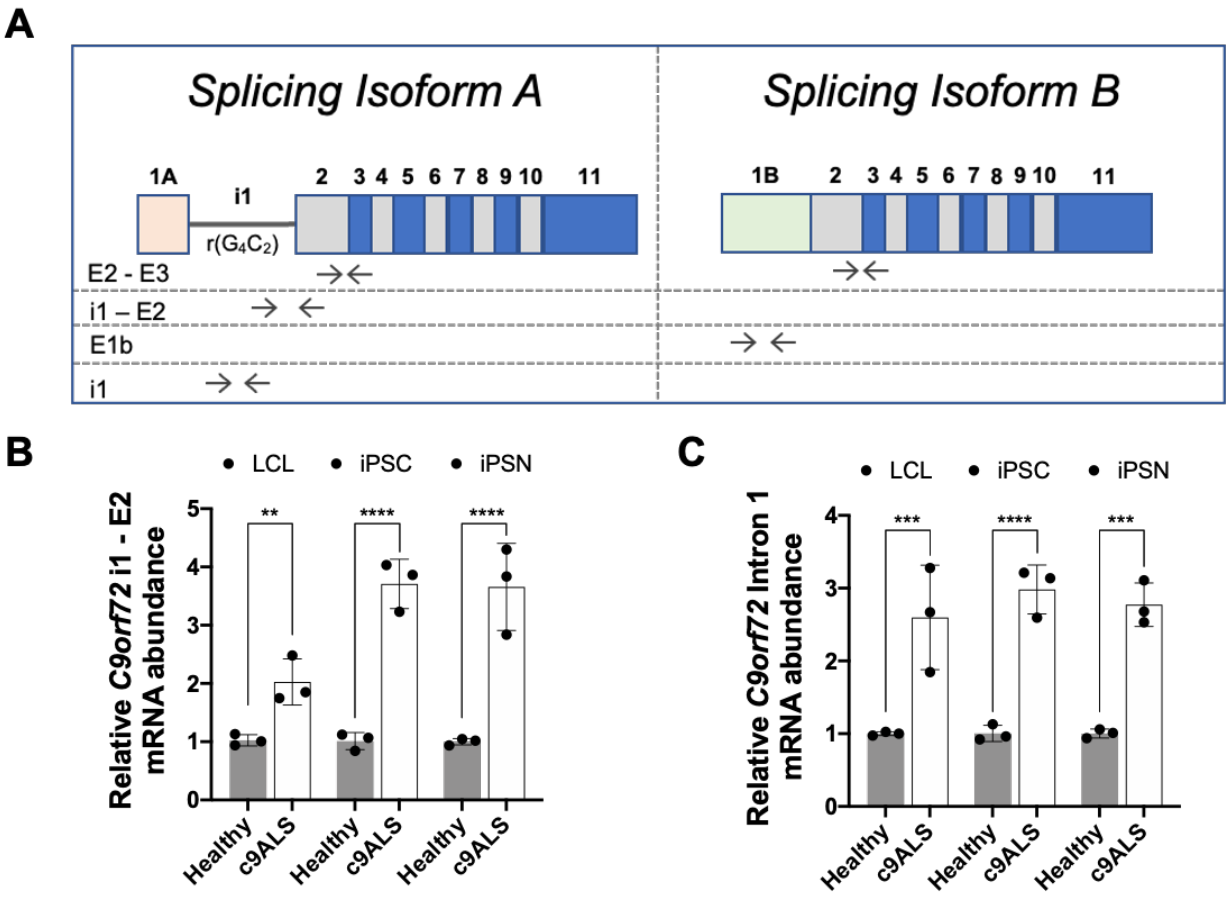

Fig. S10. Compound 1 rescues r(G_4C_2) repeat-associated intron retention in *C9orf72*. **(A)** Schematic of primer sites used to measure intron retention. **(B)** Relative abundance of intron retention in healthy vs. c9ALS patient-derived cell lines, as determined by RT-qPCR using primers spanning the 3' splice site of *C9orf72* intron 1 (*C9orf72*i1) to exon2 (E2) (n = 1 line per cell type 3 replicates per line). **(C)** Relative abundance of intron retention in healthy *vs.* c9ALS patient-derived cell lines, as determined by RT-qPCR using primers located within intron 1 (n = 1 line per cell type; 3 replicates per line). RNA quantification was measured relative to *GAPDH*. Vehicle indicates 0.1% (v/v) DMSO. **P < 0.01, ***P < 0.001 , ****P < 0.0001, as determined by an unpaired t-test with Welch's correction (Panels B and C). Error bars indicate SD.

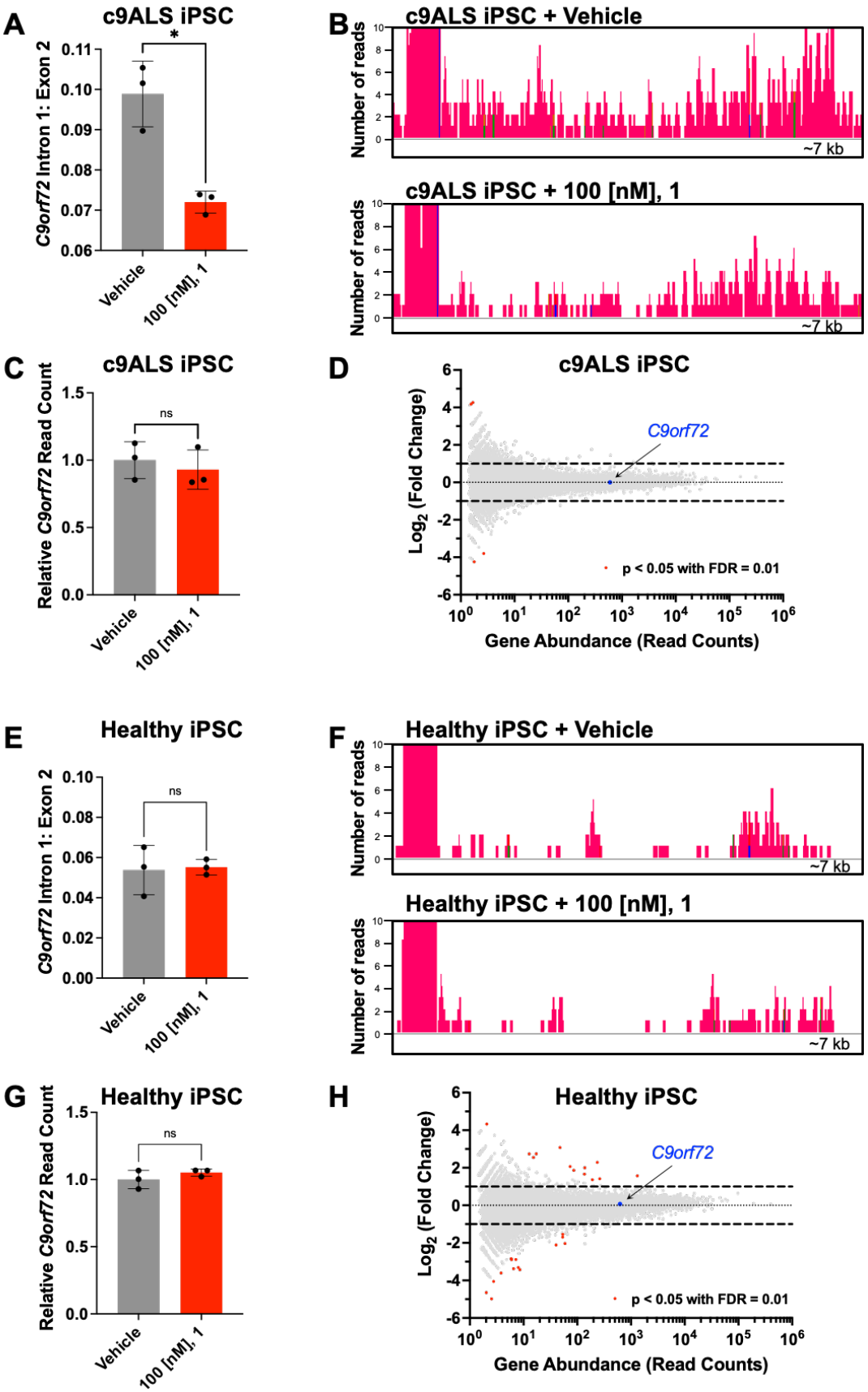
A
c9ALS iPSC
C9orf72 Intron 1: Exon 2
0.11
0.10
0.09
0.08
0.07
0.06
*
Vehicle
100 [nM], 1
B
c9ALS iPSC + Vehicle
Number of reads
~7 kb
c9ALS iPSC + 100 [nM], 1
Number of reads
~7 kb
C
c9ALS iPSC
Relative C9orf72 Read Count
1.5
1.0
0.5
0.0
ns
Vehicle
100 [nM], 1
D
c9ALS iPSC
Log2 (Fold Change)
C9orf72
p < 0.05 with FDR = 0.01
Gene Abundance (Read Counts)
E
Healthy iPSC
C9orf72 Intron 1: Exon 2
0.10
0.08
0.06
0.04
0.02
0.00
ns
Vehicle
100 [nM], 1
F
Healthy iPSC + Vehicle
Number of reads
~7 kb
Healthy iPSC + 100 [nM], 1
Number of reads
~7 kb
G
Healthy iPSC
Relative C9orf72 Read Count
1.5
1.0
0.5
0.0
ns
Vehicle
100 [nM], 1
H
Healthy iPSC
Log2 (Fold Change)
C9orf72
p < 0.05 with FDR = 0.01
Gene Abundance (Read Counts)

Fig. S11. Compound 1 selectively reduces abundance of the *C9orf72* repeat-containing intron in c9ALS patient-derived iPSCs by RNA sequencing. **(A)** Ratio of *C9orf72* Intron 1 to Exon 2 as determined by RNA-seq analysis of c9ALS patient-derived iPSCs treated with 100 nM of **1** relative to vehicle (n = 1 c9ALS iPSC line, 3 replicates). **(B)** RNA-seq reads of the intron 1 region of *C9orf72* assessed in c9ALS patient-derived iPSCs treated with vehicle (Top), or 100 nM of **1** (Bottom) and presented as a skyline plot. **(C)** Number of sequencing reads of *C9orf72* in c9ALS patient-derived iPSCs treated with 100 nM of **1** normalized to vehicle-treated cells (n = 1 c9ALS iPSC line, 3 replicates). **(D)** RNA-seq analysis of c9ALS patient-derived iPSCs treated with 100 nM of **1** plotted as average Log_2(Fold Change) over Log(Read Counts) (n = 1 c9ALS iPSC line, 3 replicates). *C9orf72* is highlighted in blue, genes significantly affected ($p<0.05$, FDR = 1%) highlighted in red. **(E)** Ratio of *C9orf72* Intron 1 to Exon 2 as determined by RNA-seq analysis of iPSCs from healthy donors treated with 100 nM, **1** relative to vehicle (n = 1 healthy iPSC line, 3 replicates). **(F)** RNA-seq reads of the intron 1 region of *C9orf72* assessed in iPSCs from healthy donors treated with vehicle (Top), or 100 nM of **1** (Bottom) and presented as a skyline plot. **(G)** Number of sequencing reads of *C9orf72* in iPSCs from healthy donors treated with 100 nM of **1** normalized to vehicle-treated cells (n = 1 healthy iPSC line, 3 replicates). **(H)** RNA-seq analysis of iPSCs from healthy donors treated with 100 nM of **1** plotted as average Log_{10}(TPM) (n = 1 healthy iPSC line, 3 replicates). *C9orf72* is highlighted in blue, genes significantly affected ($p<0.05$, FDR = 1%) highlighted in red.

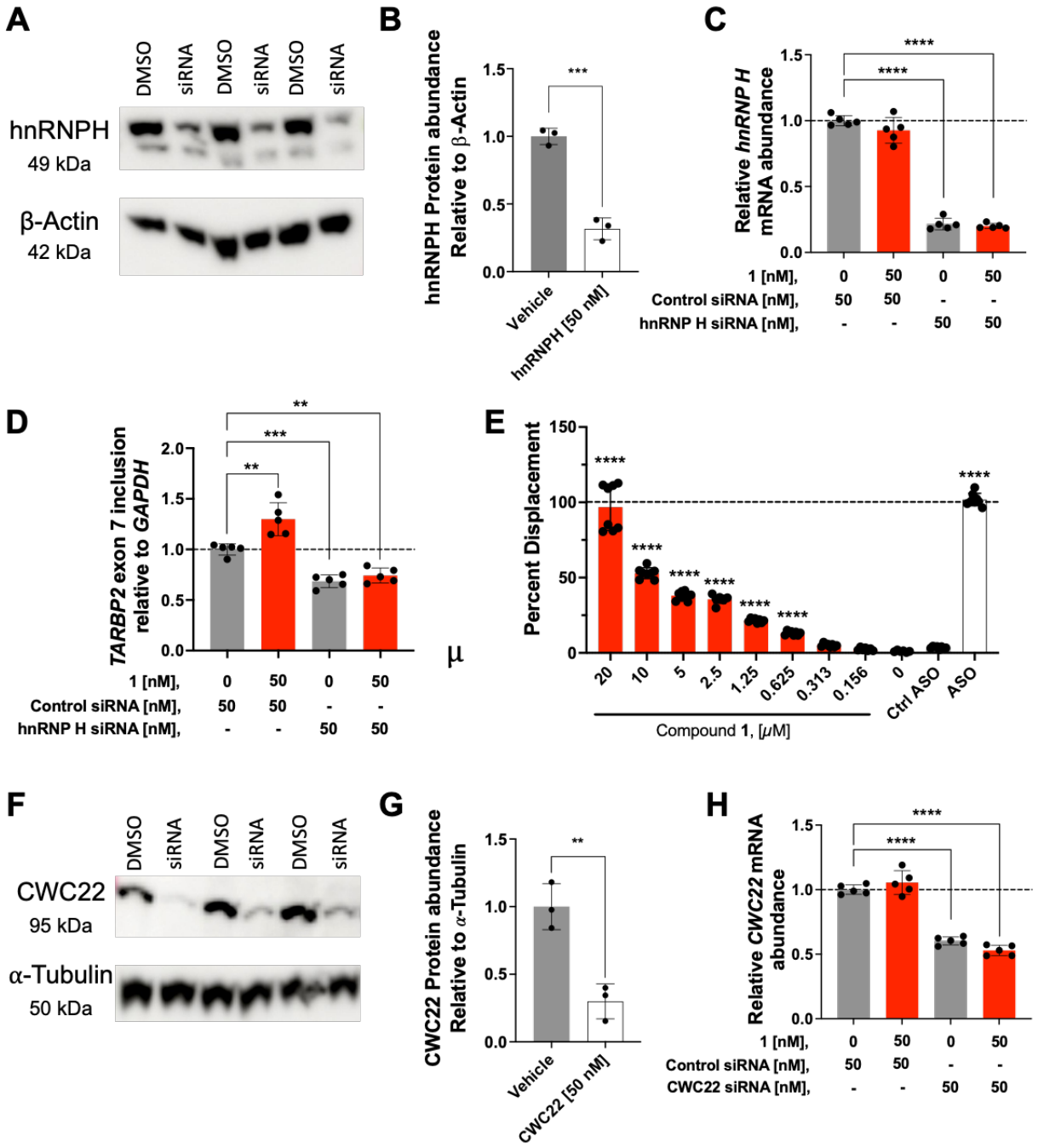

Fig. S12. siRNA knock down of the splicesome and RNA-binding protein hnRNP H in c9ALS patient-derived iPSCs at the RNA and protein levels. **(A)** Representative Western blot showing hnRNP H and β-actin protein levels upon treatment of 50 nM of *hnRNP H*-targeting siRNA pool in c9ALS patient-derived iPSCs. **(B)** Quantification of hnRNP H knockdown (normalized to β-actin) upon treatment with *hnRNP H*-targeting siRNA pool (n = 1 c9ALS iPSC line, 3 replicates). **(C)** RT-qPCR analysis confirming knockdown of *hnRNP H* transcripts upon treatment with *hnRNP H*-targeting siRNA pool (n = 1 c9ALS iPSC line, 5 replicates). **(D)** RT-qPCR analysis showing *TARBP2* exon 7 inclusion is increased when hnRNP H is liberated by **1**, allowing for hnRNP H to carry out its canonical role in *TARBP2* pre-mRNA splicing (n = 1 c9ALS iPSC line, 5 replicates). **(E)** TR-FRET analysis reported as percent displacement of hnRNP H - His_6 from a 5′-biotin-r$(G_4C_2)_8$ hairpin. Binding is quantified using an anti-His_6 antibody labeled with Tb that binds

to hnRNP H (ex: 345 nm; em: ~545 nm), along with a streptavidin XL665 (ex: 545 nm; em: 665 nm) that binds to 5′-biotin-r$(G_4C_2)_8$. FRET is calculated as fluorescence intensity at 665 nM (FRET) divided by the fluorescence intensity at 545 nM (Tb), both excited with 345 nm light. **(F)** Representative Western blot showing CWC22 and α-tubulin protein levels upon treatment of 50 nM of *CWC22*-targeting siRNA in c9ALS patient-derived iPSCs. **(G)** Quantification of CWC22 knockdown (normalized to α-tubulin) upon treatment with *CWC22*-targeting siRNA (n = 1 c9ALS iPSC line, 3 replicates). **(H)** RT-qPCR analysis confirming knockdown of *CWC22* transcripts upon treatment with *CWC22*-targeting siRNA (n = 1 c9ALS iPSC line, 5 replicates). Vehicle indicates 0.1% (v/v) DMSO. **P < 0.005, ***P < 0.001 , and ****P < 0.0001, as determined by an unpaired t-test (Panels B, C, D, G, & H) or a one way ANOVA with multiple comparisons (Panel E). Error bars indicate SD.

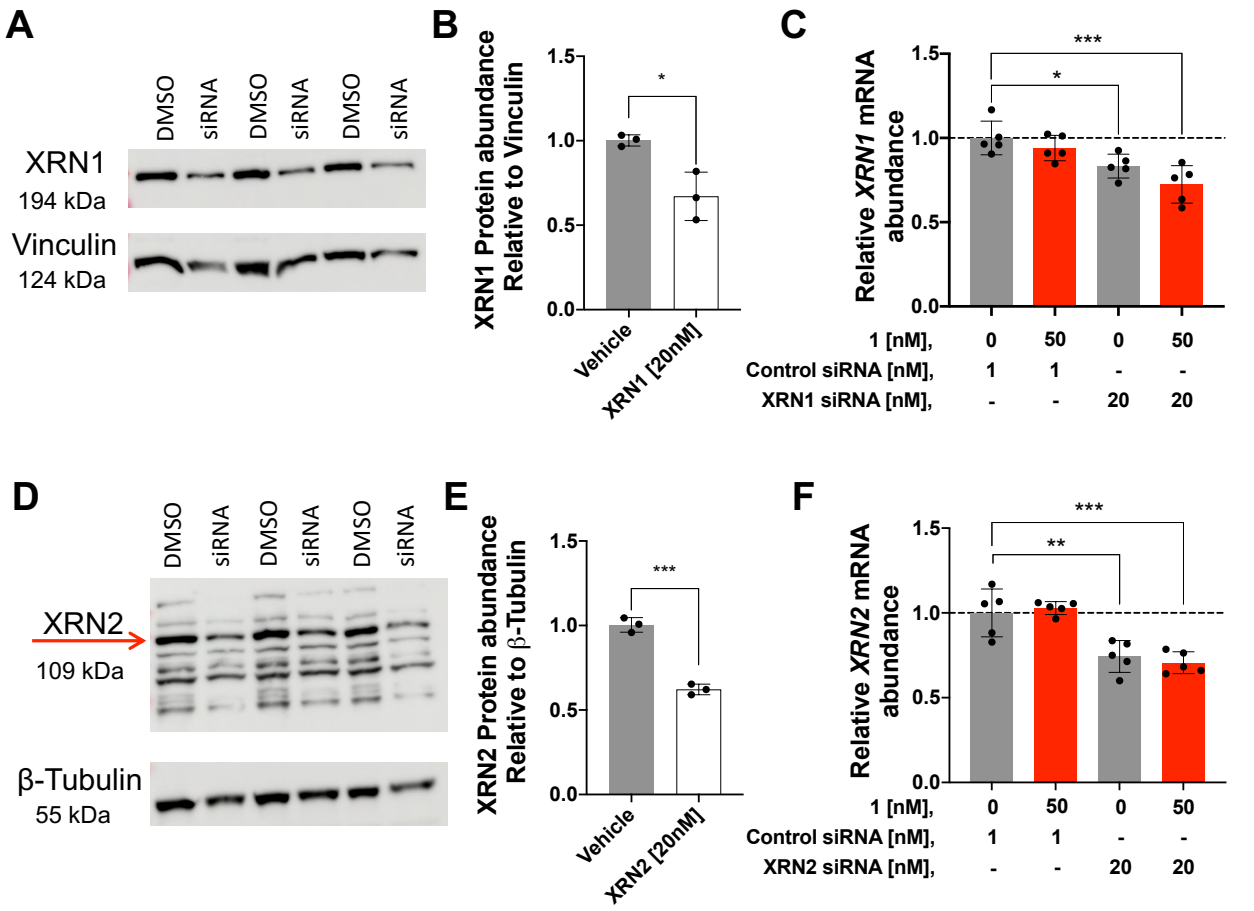

Fig. S13. siRNA knock-down of ribonucleases XRN1 and XRN2 in c9ALS patient-derived iPSCs at the RNA and protein level. (A) Representative Western blot showing XRN1 and vinculin protein levels upon treatment of 20 nM of *XRN1*-targeting siRNA pool in c9ALS patient-derived iPSCs. **(B)** Quantification of XRN1 knockdown (normalized to vinculin) upon treatment with *XRN1*-targeting siRNA pool (n = 1 c9ALS iPSC line, 3 replicates). **(C)** RT-qPCR analysis confirming knockdown of *XRN1* transcripts upon treatment with *XRN1*-targeting siRNA pool (n = 1 c9ALS iPSC line, 5 replicates). **(D)** Representative Western blot showing XRN2 and β-tubulin protein levels upon treatment of 20 nM of *XRN2*-targeting siRNA pool in c9ALS patient-derived iPSCs. **(E)** Quantification of XRN2 knockdown normalized to β-tubulin) upon treatment with *XRN2*-targeting siRNA pool (n = 1 c9ALS iPSC line, 3 replicates). **(F)** RT-qPCR analysis confirming knockdown of *XRN2* transcripts upon treatment with *XRN2*-targeting siRNA pool (n = 1 c9ALS iPSC line, 5 replicates). RNA quantification was measured relative to *GAPDH*. Vehicle indicates 0.1% (v/v) DMSO. *P < 0.05, **P < 0.01, and ***P < 0.001, as determined by an unpaired t-test (Panels B-C and E-F). Error bars indicate SD.

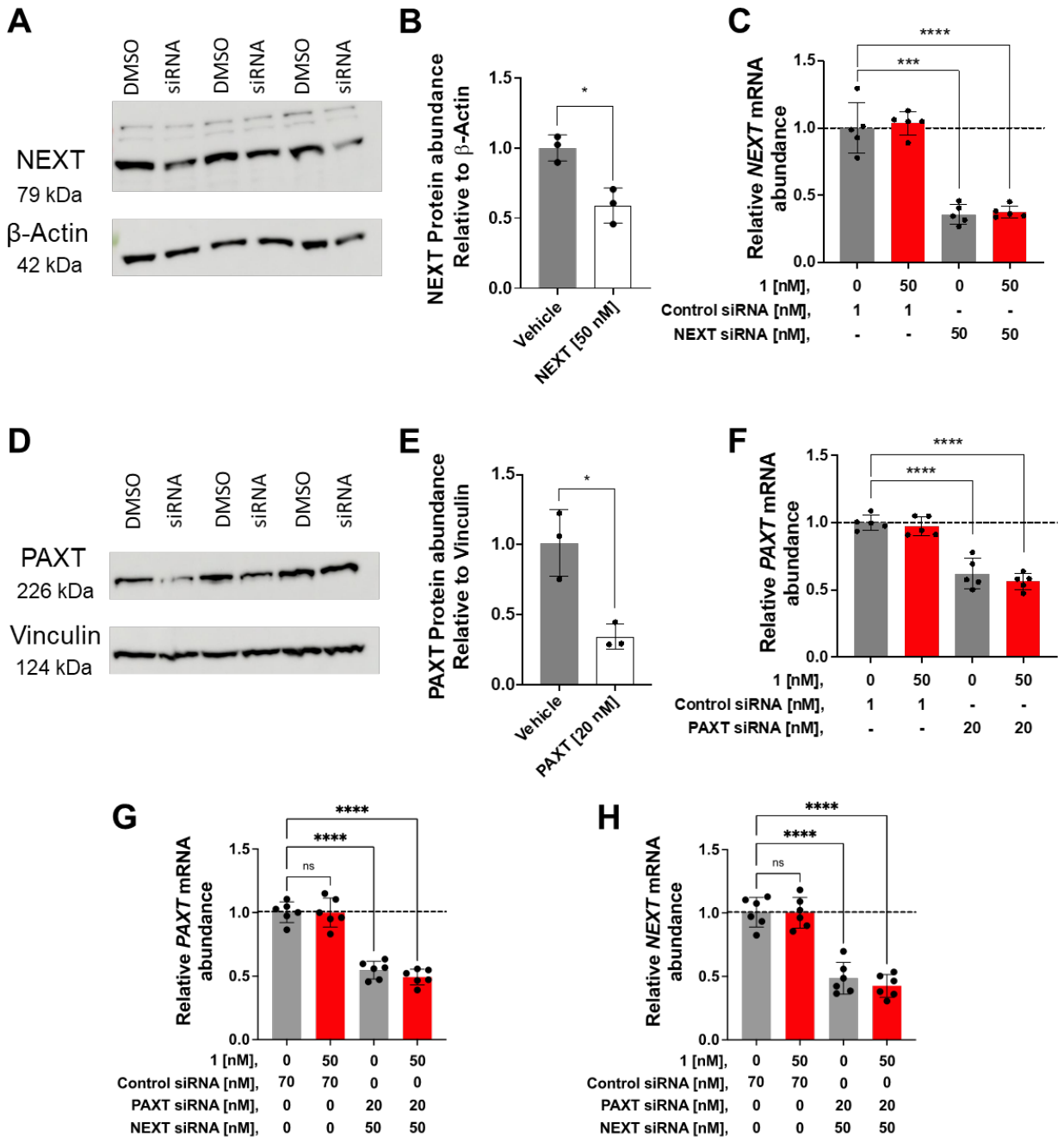

Fig. S14. siRNA knock down of the nuclear exosome adaptor proteins PAXT and NEXT in c9ALS patient-derived iPSCs at the RNA and protein levels. **(A)** Representative Western blot showing NEXT and β-actin protein levels upon treatment of 50 nM of *NEXT*-targeting siRNA in c9ALS patient-derived iPSCs. **(B)** Quantification of NEXT knockdown (normalized to β-actin) upon treatment with *NEXT*-targeting siRNA (n = 1 c9ALS iPSC line, 3 replicates). **(C)** RT-qPCR analysis confirming knockdown of *NEXT* transcripts upon treatment with *NEXT*-targeting siRNA (n = 1 c9ALS iPSC line, 5 replicates). **(D)** Representative Western blot showing PAXT and vinculin protein levels upon treatment of 20 nM of *PAXT*-targeting siRNA pool in c9ALS patient-derived iPSCs. **(E)** Quantification of PAXT knockdown (normalized to vinculin) upon treatment with *PAXT*-targeting siRNA pool (n = 1 c9ALS iPSC line, 3 replicates). **(F)** RT-qPCR analysis confirming knockdown of *PAXT* transcripts upon treatment with *PAXT*-targeting siRNA (n = 1 c9ALS iPSC line, 5 replicates). **(G)** RT-qPCR analysis confirming knockdown of *PAXT* transcripts upon co-treatment with *PAXT*-targeting siRNA pool and *NEXT*-targeting siRNA (n = 1

c9ALS iPSC line, 6 replicates). **(H)** RT-qPCR analysis confirming knockdown of *NEXT* transcripts upon co-treatment with *PAXT*-targeting siRNA pool and *NEXT*-targeting siRNA (n = 1 c9ALS iPSC line, 6 replicates). RNA quantification was measured relative to *GAPDH*. Vehicle indicates 0.1% (v/v) DMSO. *P < 0.05, **P < 0.01, ***P < 0.0001 , and ****P < 0.0001, as determined by an unpaired t-test (Panels B-C and E-I). Error bars indicate SD.

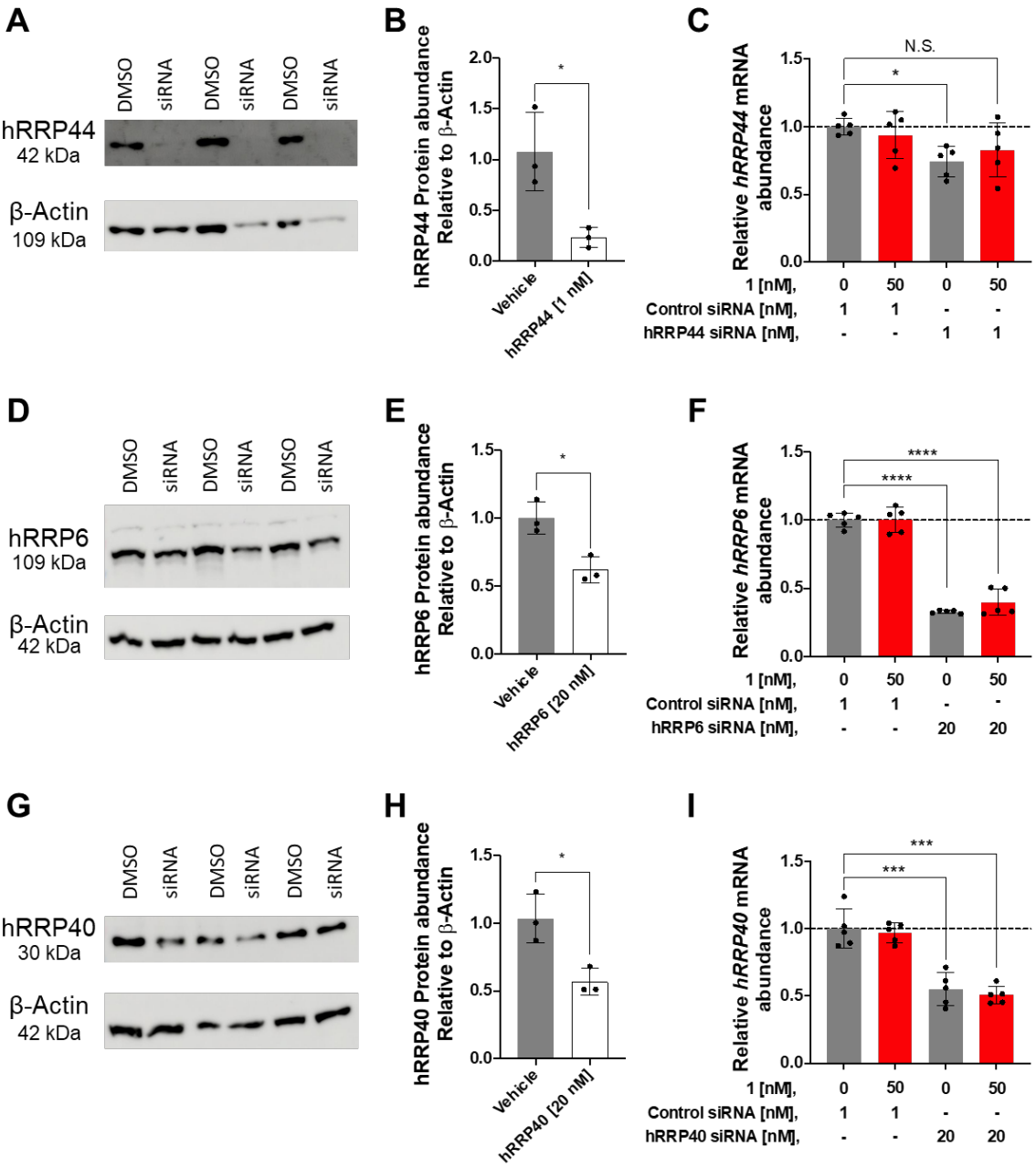

Fig. S15. siRNA knock down of various components of the cytoplasmic and nuclear exosome complex in c9ALS patient-derived iPSCs at the RNA and protein level. (A) Representative Western blot showing hRRP44 and β-actin protein levels upon treatment of 1 nM of *hRRP44*-targeting siRNA pool in c9ALS patient-derived iPSCs. **(B)** Quantification of hRRP44 knockdown (normalized to β-actin) upon treatment with *hRRP44*-targeting siRNA pool (n = 1 c9ALS iPSC line, 3 replicates). **(C)** RT-qPCR analysis confirming knockdown of *hRRP44* transcripts upon treatment with *hRRP44*-targeting siRNA pool (n = 1 c9ALS iPSC line, 5 replicates). **(D)** Representative Western blot showing hRRP6 and β-actin protein levels upon treatment of 20 nM of *hRRP6*-targeting siRNA in c9ALS patient-derived iPSCs. **(E)** Quantification of hRRP6 knockdown (normalized to β-actin) upon treatment with *hRRP6*-targeting siRNA (n = 1 c9ALS iPSC line, 3 replicates). **(F)** RT-qPCR analysis confirming knockdown of *hRRP6* transcripts upon treatment with *hRRP6*-targeting siRNA (n = 1 c9ALS iPSC line, 5 replicates). **(G)** Representative Western blot showing hRRP40 and β-actin protein levels upon treatment of 20 nM of *hRRP40*-targeting siRNA in c9ALS patient-derived iPSCs. **(H)** Quantification of hRRP40 knockdown (normalized to β-actin) upon treatment with *hRRP40*-targeting siRNA (n = 1 c9ALS iPSC line, 3 replicates). **(I)** RT-qPCR analysis confirming

knockdown of *hRRP40* transcripts upon treatment with *hRRP6*-targeting siRNA (n = 1 c9ALS iPSC line, 5 replicates). RNA quantification was measured relative to *GAPDH*. Vehicle indicates 0.1% (v/v) DMSO. *P < 0.05, ***P < 0.0001 , and ****P < 0.0001, as determined by an unpaired t-test (Panels B-C, E-F, and H-I). Error bars indicate SD.

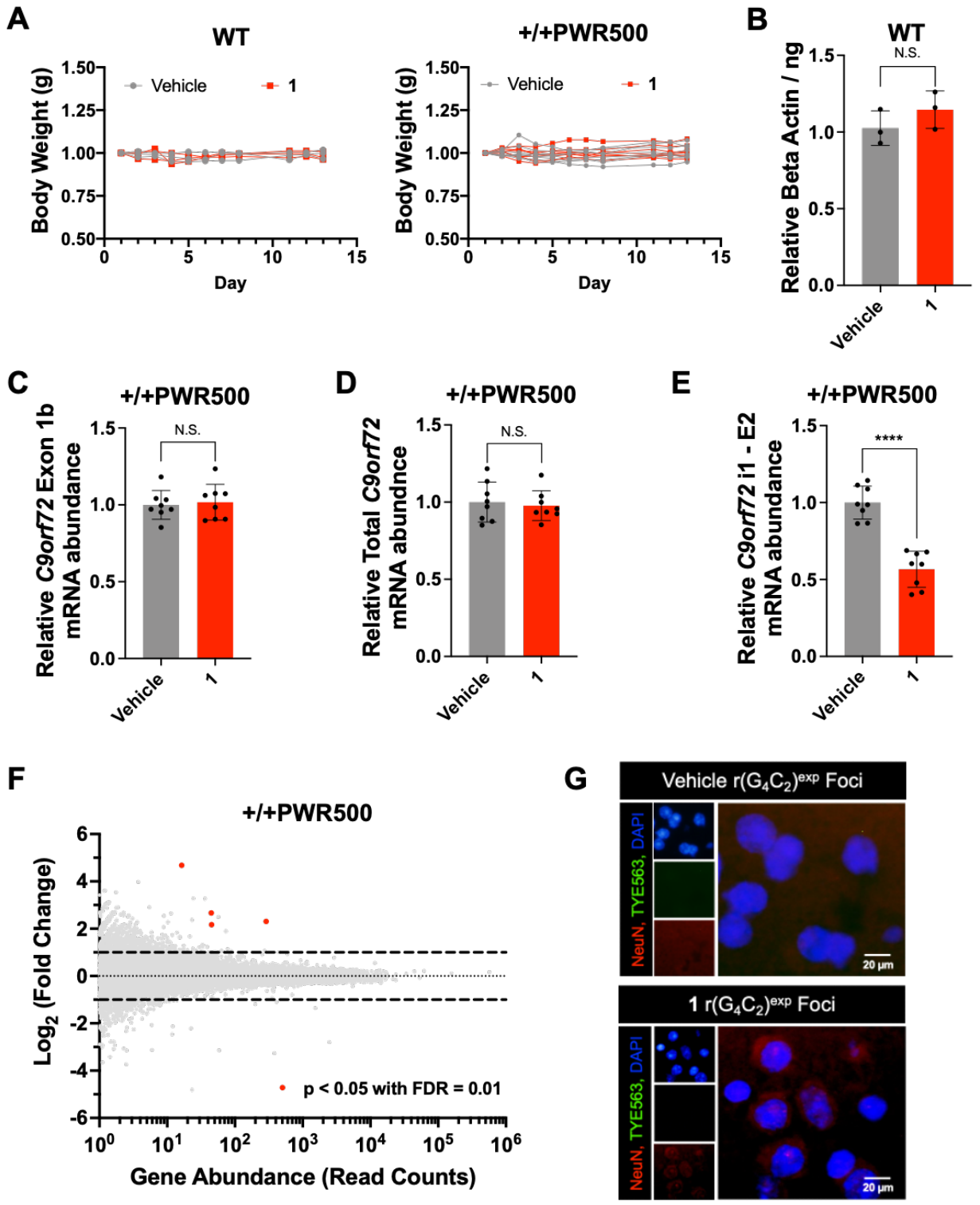

Fig. S16. Compound 1 alleviates c9ALS/FTD-associated pathology in a pre-clinical c9BAC +/+PWR500 transgenic mouse model. (A) Relative change in bodyweight of each mouse during the two-week dosing period. **(B)** Effect of **1** on the abundance of control protein β-actin in brain tissue harvested

from WT mice. Relative β-actin abundance was normalized to total protein levels and vehicle-treated mice, as determined from an electrochemical luminescence sandwich immunoassay (n = 3 mice per treatment group). **(C)** Effect of **1** on *C9orf72* exon 1b levels in +/+PWR500 mice, as determined by RT-qPCR analysis of total RNA isolated from treated and untreated mice with human C9orf72 exon 1b specific primers (n = 8 mice per treatment group). **(D)** Effect of **1** on total human *C9orf72* levels in +/+PWR500 mice, as determined by RT-qPCR analysis of total RNA isolated from treated and untreated mice with human *C9orf72* specific primers unique to the non-repeat containing isoform (n = 8 mice per treatment group). **(E)** Effect of **1** on intron 1 3' splice site ratio in +/+PWR500 mice, as determined by RT-qPCR analysis of total RNA isolated from treated and untreated mice with human C9orf72 intron 1 – exon 2 specific primers (n = 8 mice per treatment group). **(F)** RNA-seq analysis of total RNA harvested from brain tissue of +/+PWR500 mice treated with **1** compared to vehicle, plotted as average Log_2(Fold Change) over Log(Read Counts) (n = 5 mice per treatment group). Genes significantly affected ($p<0.05$, FDR = 1%) are highlighted in red. **(G)** Representative images of $r(G_4C_2)^{exp}$ foci by RNA FISH in the cortex from WT mice treated with **1** or vehicle (n = 3 mice per treatment group). $r(G_4C_2)^{exp}$ foci are absent in WT mice lacking the expanded repeat. *$P < 0.05$, as determined by an unpaired t-test with Welch's correction (Panel E). Error bars indicate SD.

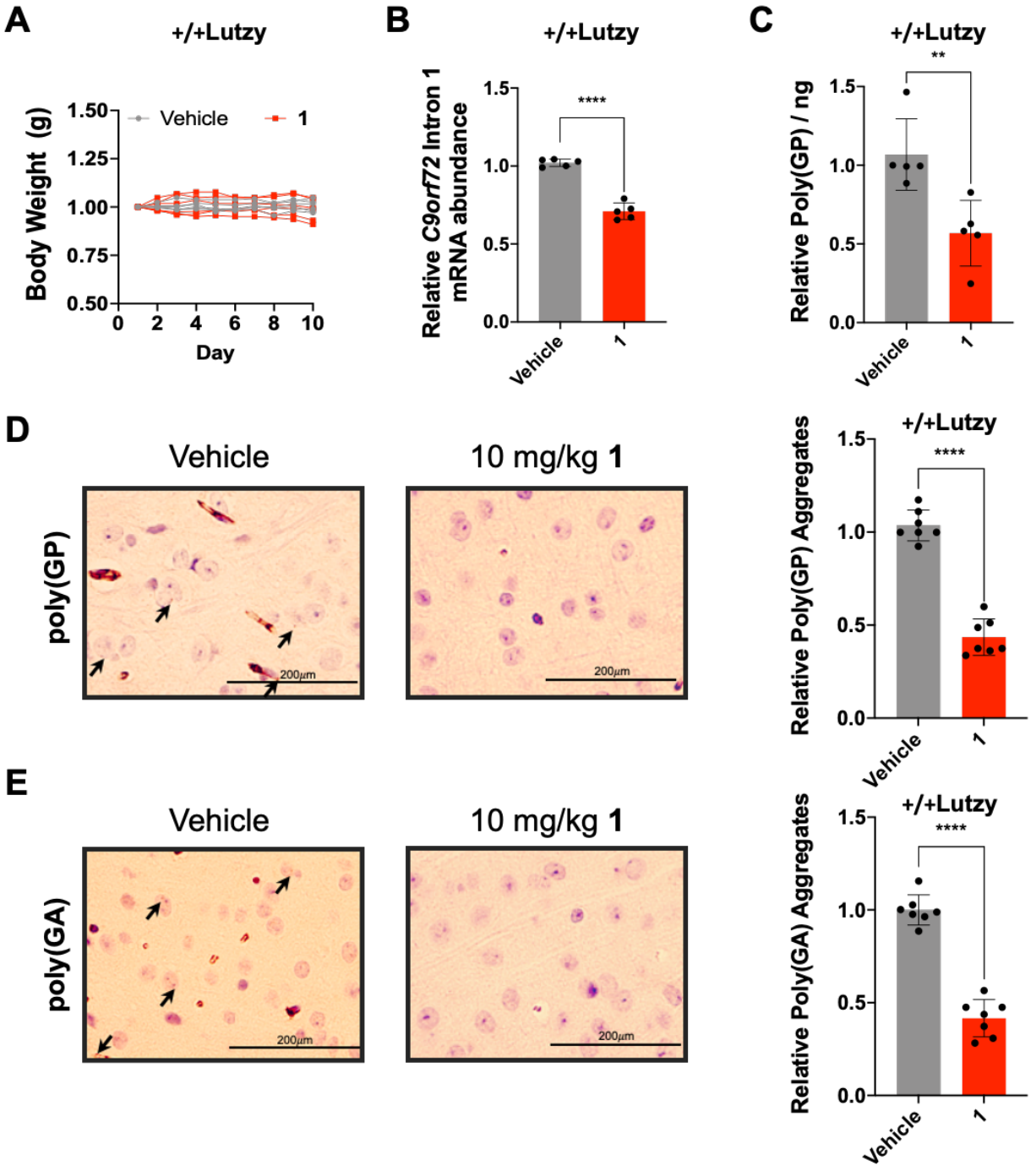

Fig. S17 Compound 1 alleviates c9ALS/FTD-associated pathology in the Lutzy c9BAC transgenic mouse model. **(A)** Relative change in bodyweight of each mouse during the 2-week dosing period. **(B)** Effect of **1** on r(G_4C_2)^{exp}-containing intron 1 levels in the Lutzy *C9orf72* BAC mouse model, as determined by RT-qPCR analysis of total RNA isolated from treated and untreated mice with intron 1-specific primers (n = 5 mice per treatment group). **(C)** Effect of **1** on poly(GP) abundance in brain tissue harvested from Lutzy mice, as determined from an electrochemical luminescence sandwich immunoassay. Relative poly(GP) abundance was normalized to total protein levels and vehicle-treated mice (n = 5 mice per treatment group). **(D)** Left**:** Representative histological images of cortex from Lutzy mice treated with **1** or

vehicle, visualizing poly(GP) aggregates. Arrows point to poly(GP) punctate. Right**:** Quantification of poly(GP) aggregates from histological analysis (n = 5 mice per treatment group; 200 cells counted per section). **(E)** Left**:** Representative histological images of cortex from Lutzy mice treated with **1** or vehicle, visualizing poly(GA) aggregates. Arrows point to poly(GA) punctate Right**:** Quantification of poly(GA) aggregates from histological analysis (n = 5 mice per treatment group; 200 cells counted per section). **P < 0.01 , ****P < 0.0001, as determined by an unpaired t-test with Welch's correction (Panels B-E). Error bars indicate SD.

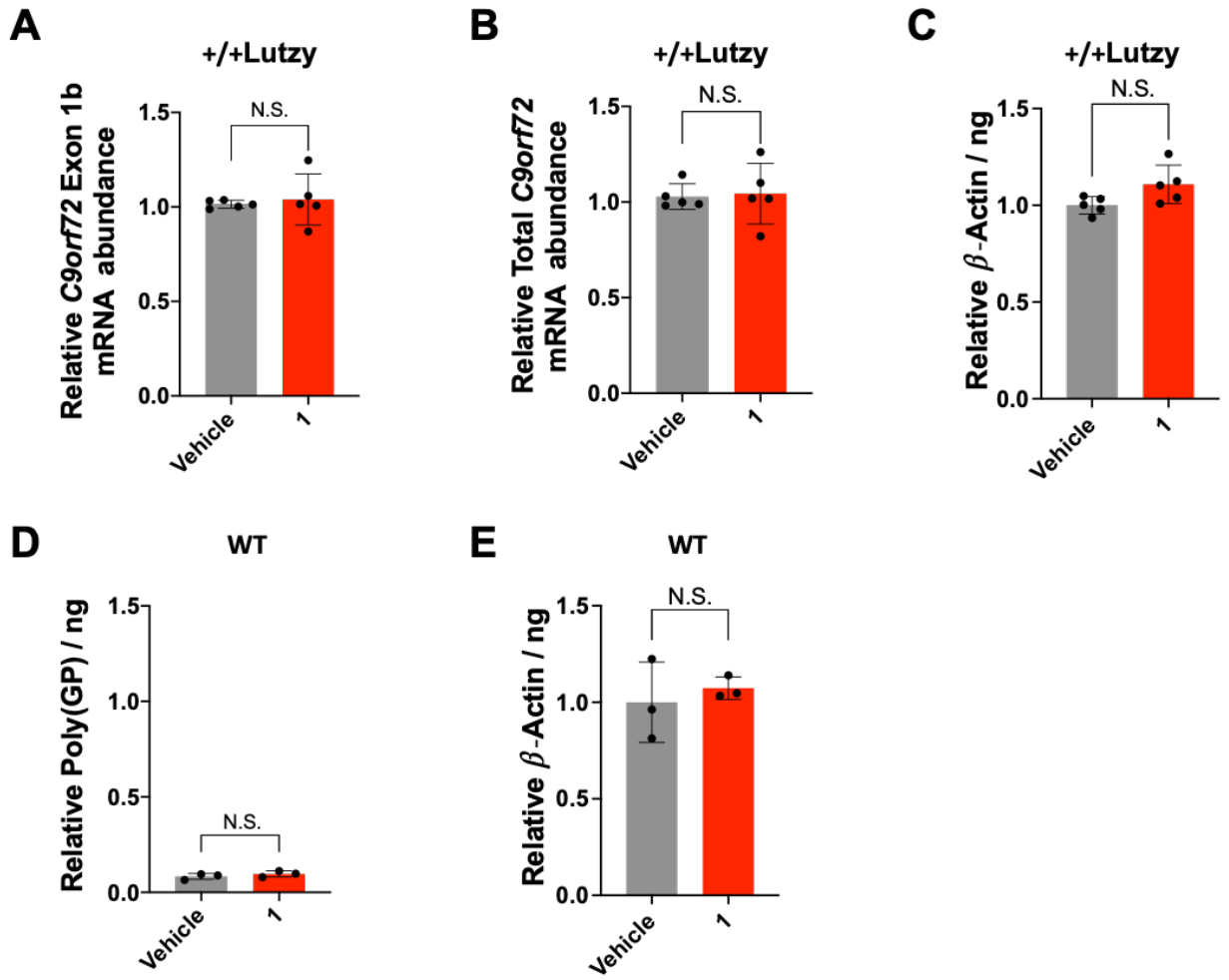

Fig. S18. Compound 1 demonstrates selectivity in the Lutzy c9BAC transgenic mouse model. **(A)** Effect of **1** on *C9orf72* exon 1b levels, contained in transcripts lacking r(G_4C_2)^{exp}, in Lutzy mice, as determined by RT-qPCR analysis of total RNA isolated from treated and untreated mice with exon 1b-specific primers (n = 5 mice per treatment group). **(B)** Effect of **1** on total human *C9orf72* exon levels in Lutzy mice, as determined by RT-qPCR analysis of total RNA isolated from treated and untreated mice with human *C9orf72* specific primers unique to the non-repeat containing isoform (n = 5 mice per treatment group). **(C)** Effect of **1** on the abundance of control protein β-actin abundance in brain tissue harvested from Lutzy mice, as determined from an electrochemical luminescence sandwich immunoassay. Relative β-actin abundance was normalized to total protein levels and vehicle-treated mice (n = 5 mice per treatment group). **(D)** Effect of **1** on poly(GP) abundance in brain tissue harvested from WT mice, as determined from an electrochemical luminescence sandwich immunoassay. Relative poly(GP) abundance was normalized to total protein levels and vehicle-treated mice (n = 3 mice per treatment group). **(E)** Effect of **1** on the abundance of control protein β-actin abundance in brain tissue harvested from WT mice, as determined from an electrochemical luminescence sandwich immunoassay. Relative β-actin abundance was normalized to total protein levels and vehicle-treated mice (n = 3 mice per treatment group).

Table S1. Sequences of oligonucleotides used in this study.

Oligonucleotide	**Sequence (5' to 3')**
Cy5-r$(G_4C_2)_2$	Cy5-GGGGCCGGGGCC
Cy5-r$(G_4C_2)_8$	Cy5-GGGGCCGGGGCCGGGGCCGGGGCCGGGGCCGGGGCCGGGGCCGGGGCC
Cy5-r$(G_2C_4)_4$	Cy5-GGCCCCGGCCCCGGCCCCGGCCCC
Cy5-r$(UG_3C_2)_4$	Cy5-UGGGCCUGGGCCUGGGCCUGGGCC
Cy5-r$(G_2C_2)_8$	Cy5-GGCCGGCCGGCCGGCCGGCCGGCCGGCCGGCC
Cy5-r$(CGG)_{16}$	Cy5-GGCGGCGGCGGCGGCGGCGGCGGCGGCGGCGGCGGCGGCGGCGGC
Cy5-r$(GGC)_{16}$	Cy5-GGCGGCGGCGGCGGCGGCGGCGGCGGCGGCGGCGGCGGCGGCGGC
Cy5-d$(G_4C_2)_8$	Cy5-GGGCCGGGGCCGGGGCCGGGGCCGGGCCGGGGCCGGGGCCGGGGCC
FISH Probe	TYE563-CCCCGGCCCCGGCCCC-TYE563

Table S2. Sequences of primers used in this study.

Primer	Sequence (5' to 3')
GFP (fwd)	GCACGACTTCTTCAAGTCCGCCATGCC
GFP (rev)	GCGGATCTTGAAGTTCACCTTGATGCC
β-actin (fwd)	GATTACTGCTCTGGCTCCTAGCA
β-actin (rev)	GCTCAGGAGGAGCAATGATCTT
18S (fwd)	GTAACCCGTTGAACCCCATT
18S (rev)	CCATCCAATCGGTAGTAGCG
TATA Binding Box (fwd)	TGCACAGGAGCCAAGAGTGAA
TATA Binding Box (rev)	CACATCACAGCTCCCCACCA
C9orf72 exon 2-3 (fwd)	ACTGGAATGGGGATCGCAGCA
C9orf72 exon 2-3 (rev)	ACCCTGATCTTCCATTCTCTCTGTGCC
C9orf72 intron 1 (fwd)	ACGCCTGCACAATTTCAGCCCAA
C9orf72 intron 1 (rev)	CAAGTCTGTGTCATCTCGGAGCTG
C9orf72 i1-e2 (fwd)	CATTTGGGGTTTTGATGGAT
C9orf72 i1-e2 (rev)	GTCCATATGTGCTGCGATCC
C9orf72 exon 1b (fwd)	TGTGACAGTTGGAATGCAGTGA
C9orf72 exon 1b (rev)	GCCACTTAAAGCAATCTCTGTCTTG
CWC22 (fwd)	GAAACACTCGGTTTGCCATCAAC
CWC22 (rev)	CTGGTTTCTGCGCCACAATGAC
hnRNP H (fwd)	GAGGGATTCGTGGTGAAGG
hnRNP H (rev)	TCCACCGGCAATGTTATCC
TARBP2 (fwd)	CACAGTGACCCAGGAGTCTG
TARBP2 (fwd)	TCGTAGAGAATCCCAGGTGC
hRRP6 (fwd)	CTCTTTGGACCTCACGACTGCT
hRRP6 (rev)	AAGAAGCTCGCCTGCTTCTGAA
hRRP40 (fwd)	GGTGTCATTGGACAGGATGGTC
hRRP40 (rev)	TCTCCAGTGGATAGAGTTTTCCC

hRRP44 (fwd)	ACCCTCACTTAAAATAGAAGATACAGT
hRRP44 (rev)	CCATTAAGGTCCATGTTTGAAGT
NEXT (fwd)	CCTCGGAATGCTGCTCGAAT
NEXT (rev)	GTGCATCTTGAAGTTCCTCA
PAXT (fwd)	ATGGAGAAGAGCTTGCTCGG
PAXT (rev)	GCCCAAAGCGATCTTGTTCC
XRN1 (fwd)	CCAGCAAAGCAGTCGTGGAGAA
XRN1 (rev)	CCACGACTCTAGCTTCCTCAAG
XRN2 (fwd)	CCCAAACCATGTGGTCTTTGTAATC
XRN2 (rev)	TGGTAGGCTGGCCATTGTGA
Mouse β-actin (fwd)	AGGTATCCTGACCCTGAAG
Mouse β-actin (rev)	GCTCATTGTAGAAGGTGTGG
Human C9orf72 insert (fwd)	TCTCCAGCTGTTGCCAAGAC
Human C9orf72 insert (rev)	TCCATTCTCTCTGTGCCTTCT
Exosome c10 (fwd)	CTCTTTGGACCTCACGACTGCT
Exosome c10 (rev)	AAGAGGCTCGCCTGCTTCTGAA

Table S3. Sequences of ASOs and siRNA used in this study.

Name	Sequence (5' to 3')[a] or Catalog
G_4C_2-ASO	mG*mG*mC*C*C*C*G*G*C*C*C*C*G*G*C*C*C*mC*mG*mG
C9orf72-ASO	mU*mA*mC*A*G*G*C*T*G*C*G*G*T*T*G*T*T*mU*mC*mC
Control-ASO	mC*mC*mU*T*C*C*C*T*G*A*A*G*G*T*T*C*C*mU*mC*mC
hrRp6	G C A A A A U C U G A A A C U U U C C dT dT
hrRp40	C A C G C A C A G U A C U A G G U C A dT dT
NEXT	G G A A U G U A C C U C A G G A U A A dT dT
hrRp44/DiS3	Catalog# J-015405-11-0002
PAXT	Catalog# J-020839-17-0010
CWC22	Catalog# L-023101-02-0005
hnRNPH1	Catalog# L-012107-00-0005
XRN1	Catalog# J-013754-11-0002
XRN2	Catalog# J-017622-09-0002
Control	Catalog# D-001810-04-05

[a] m indicates 2'-O-methyl residue; * indicates LNA residue

siRNAs purchased from Horizon Discovery Biosciences

Table S4. Compounds from the Calibr's ReFRAME library that selectively inhibit RAN translation of $r(G_4C_2)^{exp}$.

Name	Compound #	% RANT	CNS-MPO	% RANT/CNS-MPO
S-16020-2	**1**	22	4.45	4.9
SN-22995	**8**	31	5.23	6.0
ZSTK-474	**9**	40	5.16	7.8
LY-3023414	**10**	44	5.37	8.1
TOP 53	**11**	42	4.58	9.3
Panobinostat lactate	**12**	46	4.34	10.6
773U82	**13**	52	4.68	11.2
(R)-MLN 576	**14**	45	4.01	11.2
(S)-MLN 576	**15**	45	4.01	11.3

Table S5. Cell line demographic metadata and the corresponding figures in which they were used.

Identifier	Cell Type	Diagnosis	Sex	Age	Source	Experiments
CRL-3216	HEK293T	Control	Female	Fetus	ATCC	S1B-C, S2A-C
ND11583	LCL	*C9orf72* (~500 repeats)	Male	59	Coriell	2A, 2D, 2G, 3B, S2D, S2E, S4A, S8A, S8D, S10B-C
ND12438	LCL	*C9orf72* (~450 repeats)	Male	65	Coriell	2A, 2D, S8A, S8D
ND09492	LCL	*C9orf72* (~200 repeats)	Male	52	Coriell	2A, 2D, S8A, S8D
GM07491	LCL	Healthy	Male	17	Coriell	S9A
CS0NKC	iPSC	*C9orf72*	Female	60	Cedars Sinai	2B, 2E, S8B, S8E
CS0BUU	iPSC	*C9orf72*	Female	63	Cedars Sinai	2B-C, 2E-F, S8B-C, S8E-F
CS2YNL	iPSC	*C9orf72*	Male	60	Cedars Sinai	2B-C, 2E-F, S8B-C, S8E-F
CS7VCZ	iPSC	*C9orf72*	Male	64	Cedars Sinai	2B-C, 2E-F, 2H-I, 3A, 3C-F, S4A-B, S5B, S5D-E, S7, S8B-C, S8E-H, S10B-C, S11A-D, S12A-D, S12F-H, S13, S14, S15
CS8PAA	iPSC	Healthy	Female	58	Cedars Sinai	S5D-E, S9B-F
CS9XH7	iPSC	Healthy	Male	53	Cedars Sinai	S9B, S9D-F
CS1ATZ	iPSC	Healthy	Female	60	Cedars Sinai	S9B, S9D-F
CS0002	iPSC	Healthy	Male	51	Cedars Sinai	S9B, S11E-H

Table S6. DMPK properties of compounds tested in C57Bl/6J mice.					
Compound	MPO	Time (min)	Plasma (μM)	Total Brain (μM)	HEK RANT IC_{50} (μM)
1	4.3	120	1.93	0.24	0.1
2	4.6	120	0.22	0.24	0.3
28	4.6	120	0.08	0.08	0.1
30	4.2	120	0.04	0.26	0.8

Table S7. Characteristics of +/+PWR500 c9ALS mice used in *in vivo* studies

Mouse	Sex	Genotype	Age	Treatment
1	M	(WT)	21	Compound
2	F	(WT)	20	Compound
3	M	(WT)	18	Compound
4	F	(WT)	20	Compound
5	M	(WT)	20	Compound
6	F	(WT)	18	Compound
7	M	(+/+)	21	Compound
8	M	(+/+)	21	Compound
9	F	(+/+)	21	Compound
10	F	(+/+)	21	Compound
11	M	(+/+)	21	Compound
12	F	(+/+)	20	Compound
13	M	(+/+)	18	Compound
14	F	(+/+)	18	Compound
15	M	(+/+)	18	Compound
16	M	(+/+)	18	Compound
17	F	(+/+)	18	Compound
18	M	(WT)	22	Vehicle
19	M	(WT)	20	Vehicle
20	M	(WT)	18	Vehicle
21	F	(WT)	21	Vehicle
22	F	(WT)	20	Vehicle
23	F	(WT)	18	Vehicle
24	F	(+/+)	21	Vehicle
25	M	(+/+)	21	Vehicle
26	M	(+/+)	21	Vehicle
27	M	(+/+)	21	Vehicle
28	M	(+/+)	20	Vehicle
29	M	(+/+)	18	Vehicle
30	F	(+/+)	18	Vehicle
31	F	(+/+)	18	Vehicle
32	M	(+/+)	18	Vehicle
33	M	(+/+)	19	Vehicle
34	F	(+/+)	19	Vehicle

Table S8. Characteristics of Lutzy c9ALS mice used in *in vivo* studies

Mouse	Sex	Genotype	Age	Treatment
1	F	(WT)	19	Compound
2	F	(WT)	19	Compound
3	M	(WT)	22	Compound
4	M	(WT)	22	Compound
5	F	(+/+)	22	Compound
6	F	(+/+)	22	Compound
7	M	(+/+)	19	Compound
8	M	(+/+)	19	Compound
9	F	(+/+)	19	Compound
10	F	(+/+)	16	Compound
11	M	(WT)	22	Vehicle
12	M	(WT)	22	Vehicle
13	F	(WT)	16	Vehicle
14	F	(WT)	16	Vehicle
15	F	(+/+)	22	Vehicle
16	F	(+/+)	22	Vehicle
17	M	(+/+)	19	Vehicle
18	M	(+/+)	19	Vehicle
19	F	(+/+)	19	Vehicle
20	F	(+/+)	16	Vehicle

Table S9. Comparison of activities and properties of known r(G_4C_2)^{exp}-targeting compounds. Activity data are reported from c9 patient-derived iPSCs (n = 4 lines) upon treatment with 500 nM of the indicated compound.

Compound	*C9orf72* i1	Poly(GP)	MW	QED	CNS-MPO
1	59%	48%	530.72	0.321	4.29
Dimer Binder (**3**)	NA	41%	769.94	0.061	1.00
Dimer RIBOTAC (**7**)	64%	59%	1278.49	0.009	0.62

References

1. Y. Li, M. D. Disney, Precise small Molecule degradation of a noncoding RNA identifies cellular binding sites and modulates an oncogenic phenotype. *ACS Chem Biol* **13**, 3065-3071 (2018).
2. L. Guan, M. D. Disney, Covalent small-molecule-RNA complex formation enables cellular profiling of small-molecule-RNA interactions. *Angew Chem Int Ed* **52**, 10010–10013 (2013).
3. S. Moore *et al.*, ADAR2 mislocalization and widespread RNA editing aberrations in C9orf72-mediated ALS/FTD. *Acta Neuropathol* **138**, 49-65 (2019).
4. K. Zhang *et al.*, The C9orf72 repeat expansion disrupts nucleocytoplasmic transport. *Nature* **525**, 56-61 (2015).
5. A. Dobin *et al.*, STAR: ultrafast universal RNA-seq aligner. *Bioinformatics* **29**, 15-21 (2013).
6. H. Li *et al.*, The sequence alignment/map format and SAMtools. *Bioinformatics* **25**, 2078-2079 (2009).
7. Y. Liao, G. K. Smyth, W. Shi, FeatureCounts: an efficient general purpose program for assigning sequence reads to genomic features. *Bioinformatics* **30**, 923-930 (2014).
8. M. I. Love, W. Huber, S. Anders, Moderated estimation of fold change and dispersion for RNA-seq data with DESeq2. *Genome Biol* **15**, 550 (2014).
9. Z. Su *et al.*, Discovery of a biomarker and lead small molecules to target r(GGGGCC)-associated defects in c9FTD/ALS. *Neuron* **83**, 1043-1050 (2014).
10. Y. Liu *et al.*, C9orf72 BAC mouse model with motor deficits and neurodegenerative features of ALS/FTD. *Neuron* **90**, 521-534 (2016).
11. R. Besselievre, H. P. Husson, Syntheses in the ellipticine-olivacine series - a possible biogenetic model. *Tetrahedron* **37**, 241-246 (1981).
12. M. Alvarez, R. Lavilla, C. Roure, E. Cabot, J. Bosch, Studies on the synthesis of strychnos indole alkaloids - introduction of the functionalized one-carbon substitutent at C-16. *Tetrahedron* **43**, 2513-2522 (1987).
13. R. Jasztold-Howorko *et al.*, Synthesis and evaluation of 9-Hydroxy-5-Methyl-(and 5,6-Dimethyl)-6h-Pyrido[4,3-B]Carbazole-1-N-[(Dialkylamino)Alkyl]Carboxamides, a new promising series of antitumor olivacine derivatives. *J Med Chem* **37**, 2445-2452 (1994).
14. J. Janes *et al.*, The ReFRAME library as a comprehensive drug repurposing library and its application to the treatment of cryptosporidiosis. *Proc Natl Acad Sci U S A* **115**, 10750-10755 (2018).
15. Z. F. Wang *et al.*, The hairpin form of r$(G_4C_2)^{exp}$ in c9ALS/FTD is repeat-associated non-ATG translated and a target for bioactive small molecules. *Cell Chem Biol* **26**, 179-190.e112 (2019).